Molecular mechanism of CD163$^+$ tumor-associated macrophage (TAM)-derived exosome-induced cisplatin resistance in ovarian cancer ascites

Xiaohui Zhang[1], Jiapo Wang[1], Na Liu[1], Weimin Wu[1], Hong Li[2], Jinhong Chen[1], Xiaoqing Guo[1]

[1]Department of Gynaecology and Obstetrics, Shanghai First Maternity and Infant Hospital, Tongji University School of Medicine, Shanghai, China; [2]CAS Key Laboratory of Computational Biology, Shanghai Institute of Biochemistry and Cell Biology, Shanghai, China

Contributions: (I) Conception and design: X Guo; (II) Administrative support: J Chen; (III) Provision of study materials or patients: J Wang; (IV) Collection and assembly of data: N Liu; (V) Data analysis and interpretation: X Zhang; (VI) Manuscript writing: All authors; (VII) Final approval of manuscript: All authors.

Correspondence to: Xiaoqing Guo; Jinhong Chen. Shanghai First Maternity and Infant Hospital, Tongji University School of Medicine, Shanghai 201204, China. Email: guoxiaoqing@51mch.com; chenjinhong@51mch.com.

Background: Studies have found that tumor-associated macrophages (TAMs) in the malignant ascites of patients with serous ovarian cancer exhibit a mixed polarization phenotype and highly variable expression of the surface marker CD163. The exosomes secreted by mesenchymal cells can be taken up by tumor cells, affecting the malignant biological behavior of them.

Methods: Using reverse transcription-polymerase chain reaction (RT-PCR) to detect the genes expression of drug resistance related factors cancer stem cells (CSCs)/multidrug resistance (MDR)/epithelial-mesenchymal transition (EMT) after CD163$^+$ TAMs exosomes in ovarian cancer ascites co-cultured with A2780 and A2780/cis-diamminedichloroplatinum (DDP). Differences of the level of miR-221-3p expression between CD163$^+$ TAMs cells (M2) and peripheral blood mononuclear cells M0 detect by microarray screening, and bioinformatics analysis predicts that its target gene is *ADAMTS6*. Western blot (WB) and immunohistochemical detection of *ADAMTS6* expression level in epithelial ovarian cancer (EOC) clinical sample tissues, and analysis of the *ADAMTS6* expression in ovarian cancer tissues and its correlation with clinicopathological factors. WB was used to detect the expression of *AKT* pathway and downstream EMT-related molecules [*SNAIL1*, *ZEB1*, Vimentin (*VIM*)] after co-culture of CD163$^+$ TAMs exosomes with ovarian cancer cell lines A2780, A2780/DDP. WB detects the expression of *EGFR* and *TGF-β1* upstream molecules of the *AKT* signaling pathway (*AKT-pAKT*) and downstream EMT molecules (*SNAIL1*, *ZEB1*, *VIM*) after overexpression of *ADAMTS6* in A2780 and A2780/DDP.

Results: We demonstrated that after CD163$^+$ TAM exosomes were taken up by EOC cells, the highly expressed miR-221-3p could downregulate the level of *ADAMTS6*, further activate the *AKT* signaling pathway, and increase the expression of EMT transcription factors *SNAIL1* and *ZEB1* and the mesothelial marker *VIM*. Decreased expression of the epithelial marker E-cadherin induced EMT, triggering a switch to a CSC-like phenotype and MDR, thereby promoting EOC cell proliferation, adhesion, migration, and resistance. Compared with benign ovarian tumors, *ADAMTS6* expression was low in EOC tissues and was closely related to the clinical stage, age, and survival curve of ovarian cancer patients.

Conclusions: Overexpression of *ADAMTS6* reduced the IC50 of cisplatin in ovarian cancer cells. The mechanism may be related to the inhibition of EMT mediated by the *EGFR/TGF-β/AKT* pathway of EOC cells, which has potential value in the treatment of ovarian cancer.

Keywords: Ovarian cancer; cisplatin resistance; tumor-associated macrophages (TAMs); exosomes; *ADAMTS6*

Submitted Jul 27, 2022. Accepted for publication Sep 16, 2022.
doi: 10.21037/atm-22-4267
View this article at: https://dx.doi.org/10.21037/atm-22-4267

Introduction

Ovarian cancer is a common gynecological reproductive system malignant tumor with a high mortality rate, of which epithelial ovarian cancer (EOC) accounts for more than 90% of cases (1). In 2018, there were 295,000 new cases of ovarian cancer worldwide, while the number of female deaths caused by the disease was 184,000 (2). A total of 75% of cases are diagnosed at an advanced stage with extensive intra-abdominal metastases (3). Surgery combined with platinum-based chemotherapy is the main treatment for ovarian cancer. Most patients are initially sensitive to platinum-based chemotherapy, but eventually the vast majority of patients develop platinum resistance, and the 5-year survival rate is only 25–35% (4). Platinum resistance is the main reason for the poor prognosis of ovarian cancer, but its underlying mechanism has not been fully elucidated. Therefore, it is of great importance to develop more effective methods for reversing resistance.

The tumor microenvironment (TME) can support malignant biological behaviors such as tumor growth, metastasis, invasion, drug resistance, and angiogenesis (5). Tumor-associated macrophages (TAMs) are key immune cells in the TME, and TAMs have been associated with poor prognosis in breast cancer (BC), colon cancer, pancreatic cancer, and lymphoma (6-9). Regarding ovarian cancer, it was found that TAMs in malignant ascites from patients with serous ovarian cancer showed a mixed polarized phenotype and highly variable expression of the surface marker CD163, and elevated CD163 expression was associated with early disease recurrence (10). Exosomes are found in the ascites and serum of patients with ovarian cancer. Exosomes are extracellular vesicles secreted by cells, carrying genetic materials such as DNA, mRNA, miRNA, long noncoding RNA (lncRNA), circular RNA (cirRNA), protein, and lipid (11). However, the mechanism through which $CD163^+$ TAMs lead to a poor prognosis of ovarian cancer, the role of exosomes in the intracellular communication between $CD163^+$ TAMs and ovarian cancer cells, and their relationship with drug resistance have not yet been reported.

The process by which cells change from an epithelial to a mesenchymal phenotype is called epithelial-mesenchymal transition (EMT) and is important for tumor invasion and metastatic spread. Dissemination and resistance to drugs or treatments are closely related (12). EMT induces the conversion of non-cancer stem cells (CSCs) to CSCs that highly express the multidrug resistance (MDR) gene, thus establishing a link between EMT, CSCs, and drug resistance. *AKT* is a serine/threonine kinase that phosphorylates and regulates important downstream effector molecules. *AKT* activation was shown to phosphorylate and activate EMT transcription factors. However, EMT conversion and immediate manifestation of CSC characteristics by tumor cells trigger the anti-apoptotic mechanism of tumor cells. *EGFR* is an important upstream activator of *AKT* (13,14). *TGF-β* signaling is also one of the most typical pathways involved in EMT induction, occurring through the induction of other signals, such as *ERK* and *PI3K/AKT*, by *TGF-β*.

A total of 19 ADAMTS (a disintegrins and metalloproteinases with thrombospondin motifs) were classified into 4 groups based on their structural and functional similarities. These proteins share a protease domain (comprising metalloprotease and integrin-like modules) and a characteristic accessory domain that contains one or more thrombospondin type 1 motifs (15,16). Studies have shown that they are involved in various functions, such as collagen maturation, organogenesis, proteoglycan degradation, and inflammation. ADAMTS can also act as tumor suppressors or oncogenes (17,18) and regulate matrix degradation, physiological and pathological tissue remodeling, cell invasion, and metastasis. ADAMTS mutation or methylation is significantly associated with increased chemosensitivity and longer overall and progression-free survival (19). Currently, there are few studies on *ADAMTS6*; however, it has been reported that *ADAMTS6* is expressed in normal mammary myoepithelial cells, superior cervical ganglia, trigeminal ganglia, heart, and placenta under physiological conditions (20). Several recent studies have shown that *ADAMTS6* is dysregulated in certain cancers, such as BC, prolactin (PRL) tumors, colorectal cancer, and pancreatic cancer, and is associated with poor prognosis (21-23). However, there are no reports on *ADAMTS6* related to the occurrence, development, and prognosis of ovarian cancer. The results of The Cancer Genome Atlas (TCGA) database analysis indicated that *ADAMTS6* expression was downregulated 0.6- and 0.8-fold in ovarian cancer peritoneal metastatic tissues compared with that in ovarian cancer low-potential malignant tissues (GSE 9891, 2 probes). *ADAMTS6* expression decreased 0.5-fold in ovarian cancer tissue compared to normal ovarian tissue [genotype-tissue expression (GTEx)]. Few studies have shown that TAM-derived exosomes have an effect on the malignant biological behavior of ovarian cancer cells (24-29), but the role of exosomes in the intracellular communication between $CD163^+$ TAMs and ovarian cancer cells and its

relationship with cisplatin resistance has not yet been reported. We present the following article in accordance with the MDAR reporting checklist (available at https://atm.amegroups.com/article/view/10.21037/atm-22-4267/rc).

Methods

Tissues

Tissue, peritoneal fluid, and peripheral blood samples of patients with benign and malignant ovarian tumors and peripheral blood samples of normal healthy women were collected. We selected 40 patients with EOC, 40 patients with benign ovarian tumors, and 40 healthy volunteers whose peripheral blood samples were maintained in liquid nitrogen. Written informed consent was obtained from all participants. The enrolled patients had not received chemotherapy, radiotherapy, surgery, immunotherapy, or other treatments, and patients with other diseases were also excluded. They were grouped according to different ages and disease stages. The study was conducted in accordance with the Declaration of Helsinki (as revised in 2013). The study was approved by the Ethics Committee of Shanghai First Maternity and Infant Hospital, Tongji University School of Medicine (approval No. [KS1937]).

Cells

A2780 and A2780/cis-diamminedichloroplatinum (DDP) human ovarian carcinoma cell lines were purchased from the American Type Culture Collection (Shanghai, China) and cultured in Roswell Park Memorial Institute (RPMI) 1640 medium supplemented with 10% fetal bovine serum (FBS) and 1% penicillin-streptomycin at 37 ℃ and 5% CO_2. $CD163^+$ TAMs were obtained from ascites of ovarian cancer patients (Shanghai First Maternity and Infant Hospital). The patients provided written informed consent for ascites collection. Monocytes were isolated using stem cell LymphoPrep (Axis Shield PoC As, Oslo, Norway).

Preparation of tumor cell suspension

Human ovarian tumor tissue samples (≤1 g) were obtained from the patients and cut into pieces 2–4 mm in size. Next, the samples were added into 15 mL test tubes, followed by the addition of the corresponding enzyme reagent (Tumor Dissociation Kit, Becton, Dickinson and company, New Jersey, USA) according to the manufacturer's instructions. Subsequently, tubes were placed in a 37 ℃ constant temperature water bath (Eppendorf, Hamburg, Germany) (mixed evenly every 5 min) or a 37 ℃ shaker for 1 h for digestion. Cell suspensions were then filtered, centrifuged, and resuspended for downstream experiments.

Preparation of monocytes from ascites and peripheral blood

Mononuclear cells were isolated from ascites of ovarian cancer patients using lymph separation fluid. To sort $CD163^+$ TAMs, cells resuspended in cold phosphate-buffered saline (PBS) were incubated with anti-human CD11B-phycoerythrin (PE), anti-human CD163-allophycocyanin (APC), and anti-human CD68-fluorescein isothiocynate (FITC) (Invitrogen, CA, USA) at 4 ℃ for 30 min. After washing, labeled cells were subjected to flow cytometry using the BD Accuri™ C6 flow cytometer (BD Biosciences, San Jose, CA, USA) to analyze and sort $CD163^+$ TAMs. Next, $CD163^+$ TAMs were cultured in Dulbecco's modified eagle medium (DMEM) supplemented with 10% FBS and 1% penicillin-streptomycin at 37 ℃ and 5% CO_2. To simulate exosome-mediated intercellular communication between tumor cells and $CD163^+$ TAMs, an *in vitro* indirect co-culturing system was established using $CD163^+$ TAMs and A2780 and A2780/DDP cells inoculated in the upper and lower chambers, respectively, of a Corning® Transwell® cell culture insert (4-μm pore, Corning Inc., Corning, NY, USA) with a polycarbonate membrane. After 48 h of co-culturing, cells were harvested for further assays.

MTS proliferation assay

After co-culture with $CD163^+$ TAMs or transient transfection with miR-221-3p mimic/inhibitor, A2780 and A2780/DDP cells (1.5×10^3) were seeded onto 96-well plates and cultured in the presence of cisplatin (0, 3, 6, 9, 12, 18, 21, 24, 27, and 30 μg/dL for A2780; 0, 9, 18, 24, 36, 48, 72, 144, 288, and 300 μg/dL for A2780/DDP) for 5 days. Next, 3-(4,5-dimethylthiazol-2yl)-5-(3-carboxymethoxy-phenyl)-2-(4-sulfophenyl)-2H-tetrazolium (MTS) Solution Reagent (Promega Biosciences, Madison, WI, USA) was added to each well, and the plates were incubated at 37 ℃ in 5% CO_2 for 2 h. Absorbance was measured at 490 nm using a 96-well plate reader (Thermo Scientific, Varioskan LUX, USA). Six replicates per group were used in these experiments. GraphPad Prism 7 software was used to plot and determine the half maximal inhibitory concentration (IC50) value of each chemotherapeutic drug in different cells, i.e., the drug concentration for 50% cell growth inhibition.

Exosome isolation

CD163+ TAMs cells were cultured in RPMI 1640 medium with or without 10% FBS for 48 h, and the cell culture supernatant was collected; centrifugation with 2,000 rpm for 30 min to remove cells and cell debris; transfer the cell supernatant after centrifugation to a new centrifuge tube; add the exosome extraction reagent (System Biosciences) of cell supernatant in the ratio of cell supernatant: exosome isolation reagent =2:1; shake, mix the cell supernatant and exosome separation reagent, 4 degrees overnight; The precipitated exosomes were recovered by standard centrifugation at 10,000 ×g for 60 min. Discard the supernatant and resuspend the exosomes with 1× PBS; purified exosomes: transfer the harvested crude exosome particles into the upper chamber of exosome purification filter (EPF column), centrifuge at 3,000 g for 10 min at 4 ℃, and collect the liquid at the bottom of the EPF column tube after centrifugation, which is the purified exosome particles. The purified exosomes were stored in a low-temperature refrigerator at –80 ℃ for future experiments.

Cell adhesion assay

CD163+ TAM-derived exosomes were co-cultured with A2780 and A2780/DDP cells, and 24-well culture plates were coated with Matrigel for 2 h. A2780 and A2780/DDP cells were laid into the 24-hole plate coated with Matrigel, in which there was 5×10^5 cells/hole. Cells were incubated at 37 ℃ for 30 min, 1 h, and 2 h, respectively, and washed twice with PBS to remove non-adherent cells. Cells were then fixed using paraformaldehyde for 30 min, washed twice using PBS, and stained using crystal violet solution for 30 min. Finally, cells were observed under a microscope (200× magnification), and images were captured and analyzed using Image J software.

Transwell migration experiment

The cell suspension (with exosome treatment) was digested by conventional cell culture methods, and 100 μL was added to the Matrigel-coated Corning® Transwell® (Corning Inc.). Place 600 μL the medium containing 20% FBS in the lower chamber of 24-hole plate. After 48 h of conventional culture, take out the Transwell cell, discard the aerial culture medium, and wash it twice with PBS; Formaldehyde was fixed for 30 minutes, and the chamber was released and air dried; stain with 0.1% crystal violet for 30 minutes, gently wipe off the upper layer of non-migrating cells in front of them, and wash them with PBS for 3 times; three visual fields were randomly selected under a 400× microscope to observe the cells and count them (Olympus).

Reverse transcription-polymerase chain reaction (RT-PCR)

RT-PCR was used to detect changes in the expression of CSC-related factors (*POU5F1*, *NANOG*, *SOX2*), EMT-related factors [Vimentin (*VIM*), *CDH1*, *TWIST1*, *SNAIL1*, *SNAIL2*, *ZEB1*], and MDR-related factors (*ABCB1*, *ABCC1*, *ABCG2*) in A2780 and A2780/DDP cells after co-culture of CD163+ TAM-derived exosomes or transient transfection with miR-221-3p mimic/inhibitor. Total RNA extraction was performed using Trizol cell lysate (Invitrogen, USA), and cDNA was obtained using a high-capacity cDNA Reverse Transcription Kit (Takara Bio Inc., CA, USA). GAPDH was used as an internal control for miRNAs. Quantitative RT-PCR (ABI Prism 7000, Thermo Fisher Scientific) analysis was performed in duplicate for each data point using primers listed in *Table 1*.

Bioinformatics analysis

CD163+ TAMs in ovarian cancer ascites and peripheral blood M0 monocytes were used as the experimental and control group, respectively. The transcriptome differences in miRNAs between the 2 groups were compared and analyzed using gene chip technology. MiR-221-3p (105-fold), miR-132-3p (71-fold), and miR-708-5p (76-fold) were significantly increased in TAMs. Using target gene prediction and Gene Ontology (GO) analysis, it was found that the corresponding target genes of miR-221-3p, miR-132-3p, and miR-708-5p were *ADAMTS6*, *Smad4*, and *ATXNTL1*, respectively.

Western blotting

Western blotting and immunohistochemistry (IHC) were used to detect the expression of *ADAMTS6* protein in human ovarian cancer tissue samples. Additionally, the expression of *ADAMTS6* in ovarian cancer and its correlation with clinicopathological factors were analyzed. Western blotting was used to detect the expression of *AKT* pathway proteins and downstream EMT-related molecules [*SNAIL1*, *ZEB1*, *VIM*] after CD163+ TAM-derived exosomes were co-cultured with ovarian cancer cell lines A2780 and A2780/DDP. Western blotting detected the expression of *EGFR* and *TGF-β1*, upstream molecules of the AKT signaling pathway,

Table 1 The primer sequences for RT-PCR experiments

Gene	Primer sequences (5'-3')	
	Forward	Reverse
GAPDH	GGAGCGAGATCCCTCCAAAAT	GGCTGTTGTCATACTTCTCATGG
ADAMTS6	CCCTTCAACAACGACATCTGT	CCGTTCAATGCTCACTGATCT
POU5F1	GGGAGATTGATAACTGGTGTGTT	GTGTATATCCCAGGGTGATCCTC
NANOG	TTTGTGGGCCTGAAGAAAACT	AGGGCTGTCCTGAATAAGCAG
SOX2	TACAGCATGTCCTACTCGCAG	GAGGAAGAGGTAACCACAGGG
ABCB1	GGGATGGTCAGTGTTGATGGA	GCTATCGTGGTGGCAAACAATA
ABCC1	TTACTCATTCAGCTCGTCTTGTC	CAGGGATTAGGGTCGTGGAT
ABCG2	ACGAACGGATTAACAGGGTCA	CTCCAGACACACCACGGAT
Vimentin	AGTCCACTGAGTACCGGAGAC	CATTTCACGCATCTGGCGTTC
CDH1	CGAGAGCTACACGTTCACGG	GGGTGTCGAGGGAAAAATAGG
TWIST1	GTCCGCAGTCTTACGAGGAG	GCTTGAGGGTCTGAATCTTGCT
SNAIL1	TCGGAAGCCTAACTACAGCGA	AGATGAGCATTGGCAGCGAG
ZEB1	TTACACCTTTGCATACAGAACCC	TTTACGATTACACCCAGACTGC

RT-PCR, reverse transcription-polymerase chain reaction.

and downstream molecules of EMT (*SNAIL1*, *ZEB1*, *VIM*) after overexpression of *ADAMTS6* in A2780 and A2780/DDP cells. Total protein was extracted from cells and tissues using RIPA lysis buffer (Cell Signaling Technology, MA) according to the manufacturer's instructions. Proteins were separated using sodium dodecyl sulfate polyacrylamide gel electrophoresis (SDS-PAGE) and then transferred to nitrocellulose membranes. The membranes were blocked with 5% bovine serum albumin and incubated with antibodies against *ADAMTS6*, *SNAIL1*, *ZEB1*, *VIM*, *EGFR*, *TGF-β1*, (Abcam, MA; 1:1,000), and GAPDH (AB2000, Shanghai, China; 1:5,000), followed by a corresponding secondary antibody. Enhanced chemiluminescence reagent (Pierce, Rockford, IL, USA) was used to detect the antigen-antibody complex.

IHC on tissue microarray

A total of 160 EOC tissues and matched adjacent tissue microarrays were obtained from Shanghai Zhuoli Biotechnology Co., Ltd. (Zhuoli Biotechnology Co., Ltd., Shanghai, China). All tissue samples used in this study were first fixed with formalin, then paraffin embedded and sectioned (5 μm) followed by dewaxing xylene and hydration in graded ethanol solution. Finally, slides were incubated with anti-*ADAMTS6* antibody (1:150; Abcam, Cambridge, MA, UK) overnight at 4 ℃, and then incubated with secondary antibody biotinylated goat anti-rabbit serum streptavidin peroxidase conjugate for 30 min at 37 ℃. Finally, it was fixed with diaminobenzene and counterstained with hematoxylin. Interpret the report with visiopharm pathological analysis system: if there is no cell staining, score 0; if there is less than 10% of cells stained, 1 point will be given; if there are 11–50% cells stained, 2 points will be given; if 51–80% of the cells are colored, 3 points will be given; if more than 81% of the cells are colored, 4 points will be given. Second, score according to staining intensity: if there is no staining, score 0; 1 point for light yellow; if it is brown yellow, 2 points will be given; 3 points for tan. The final pathological score was calculated as: staining degree score × staining intensity score.

Plasmids, transient transfections, and cell line generation

MiR-221-3p mimics and inhibitors as well as negative control (NC) mimics and NC inhibitors were purchased from Gene Pharma (Shanghai, China). Cells were seeded in 6-well plates 1 day before transfection. On the day of transfection, 200 μL of fresh appropriate complete medium was added to the cells. A transfection mix was prepared with

1.25 μL of miR-221-3p mimics/inhibitor or *ADAMTS6* plasmids and 3 μL of Lipofectamine™ 3000 Transfection Reagent (Invitrogen, Carlsbad, CA, USA) according to the manufacturer's protocol. Subsequent assays were performed after 48 h of transfection.

Statistical analysis

All experiments were independently performed at least thrice. Statistical analysis was performed using SPSS software (version 21.0; SPSS, Chicago, IL, USA). Data are presented as the mean ± standard error of the mean. Differences between groups were assessed by the *t*-test or one-way analysis of variance with multiple comparisons. Statistical significance was set at P<0.05.

Results

The distribution of CD163+ TAMs in ovarian tumors and ascites

CD163+ TAMs were detected in the peritoneal washings of patients with EOC and patients with benign ovarian cysts using flow cytometry. The proportion of CD11b/CD68-expressing double-positive mononuclear macrophages was significantly increased in the ascites of EOC patients than in patients with benign ovarian cysts (44.1%±13.3% *vs.* 7.4%±3.6%, respectively), and the difference was statistically significant. A proportion of CD163+ TAMs among CD11b/CD68 double-positive mononuclear macrophages was detected in the tissues of EOC patients and patients with benign ovarian cysts. The infiltration of TAMs was increased in the tissues of patients with EOC compared with those of patients with benign ovarian cysts (14.3%±4.1% *vs.* 6.6%±2.6%, respectively), and the difference was statistically significant (P<0.001). The proportions of CD163+ TAMs among CD11b/CD68-expressing double-positive mononuclear macrophages in the peripheral blood of normal adult women, patients with benign ovarian cysts, and patients with EOC were 4.1%±2.3%, 5.8%±3.4%, and 9.1%±3.6%, respectively. Statistical analysis showed that the proportion of CD163+ TAMs in the peripheral blood of EOC patients was significantly higher than that in normal adult female peripheral blood and the peripheral blood of benign ovarian cyst patients (P<0.001), while the proportion of CD163+ TAMs in ascites of ovarian cancer patients was significantly higher than that in the peripheral blood of the same patients (*Figure 1*).

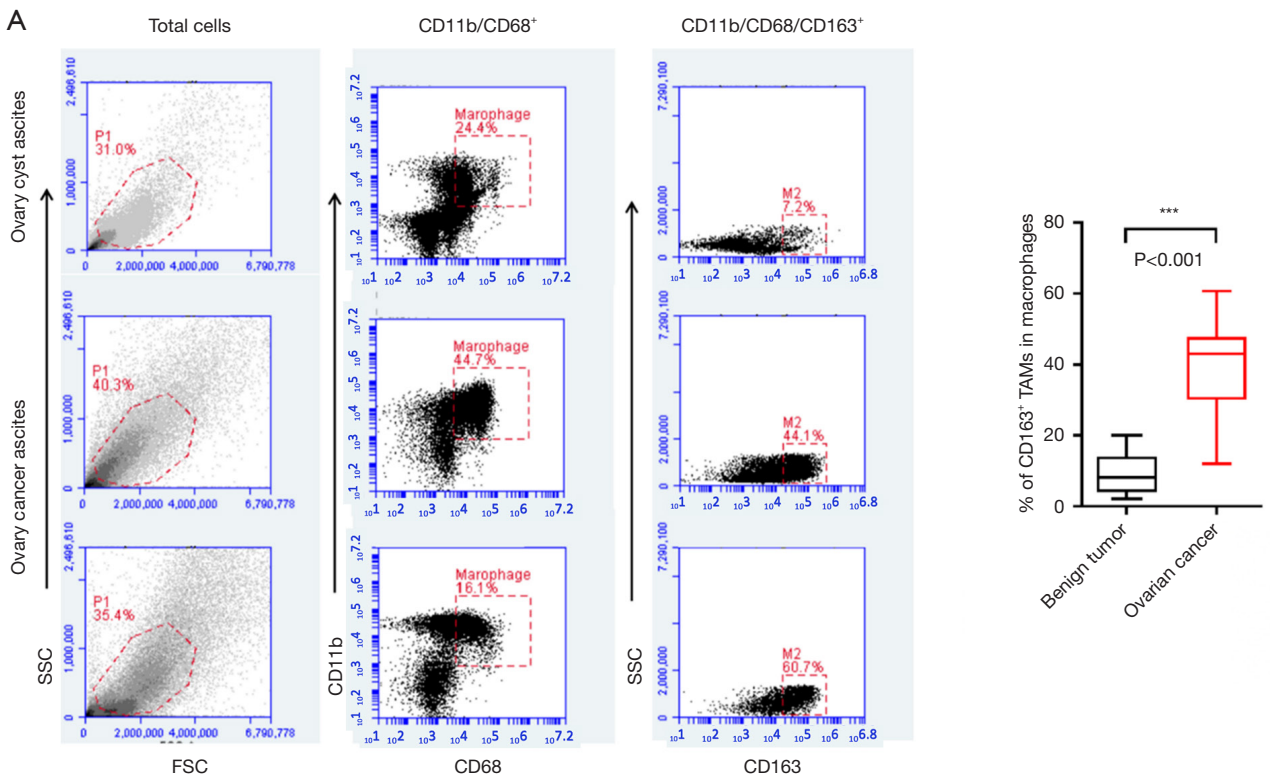

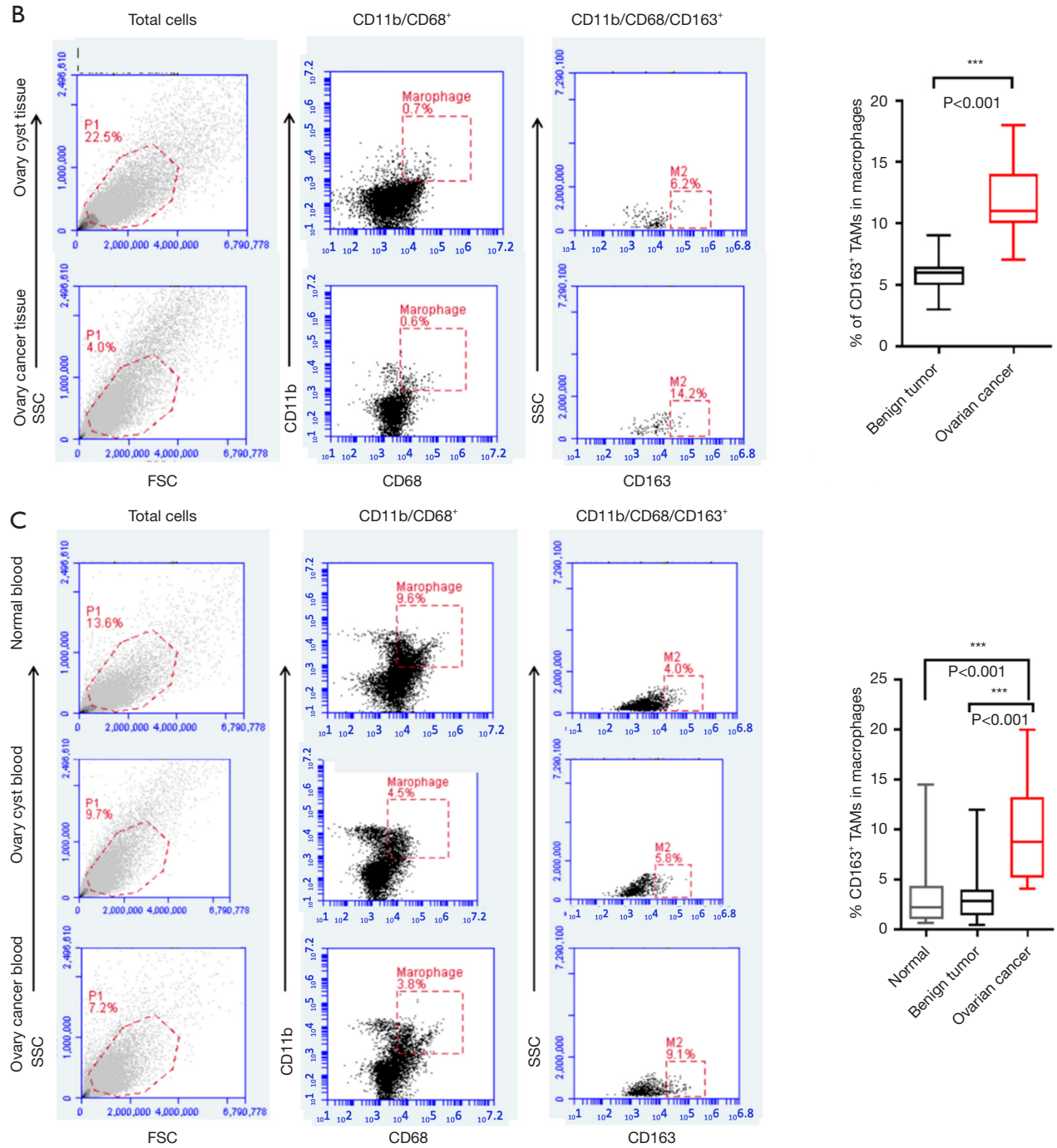

Figure 1 Distribution of CD163$^+$ TAMs in benign and malignant ovarian tumors and ascites. (A) The proportion of CD163$^+$ TAMs in CD11b/CD68 double-positive mononuclear macrophages increased significantly in ascites of epithelial ovarian cancer patients. (B) In epithelial ovarian tissues, the proportion of CD163$^+$ TAMs in CD11b/CD68 double-positive monocyte macrophages increased. (C) Compared with the peripheral blood of normal adult women and patients with benign ovarian cysts, the proportion of CD163$^+$ TAMs in the peripheral blood of patients with epithelial ovarian cancer was higher in CD11b/CD68 double-positive mononuclear macrophages; meanwhile, in patients with ovarian cancer, the proportion of CD163$^+$ TAMs in ascites was significantly higher than that in the peripheral blood of the same patient. The difference was statistically significant (n=40). ***, P<0.001. FSC, forward scatter; SSC, side scatter; TAMs, tumor-associated macrophages.

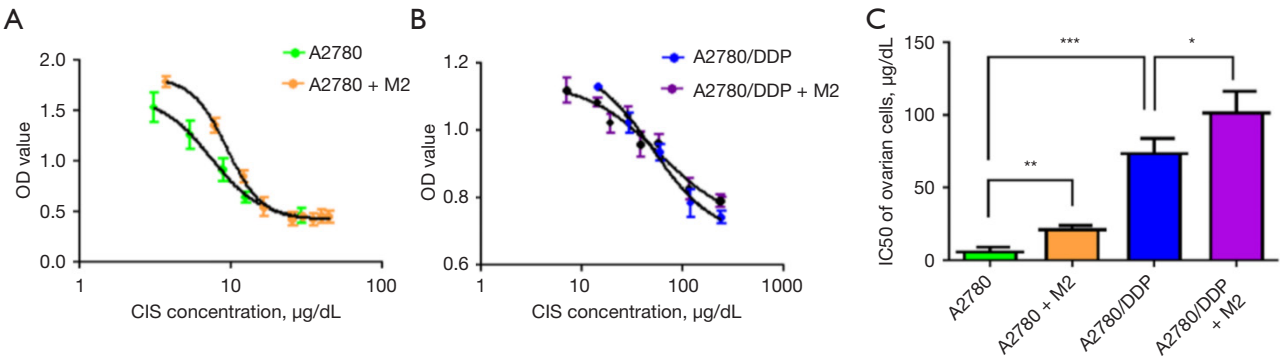

Figure 2 Effects of CD163+ TAMs on the proliferation of A2780 and A2780/DDP cells following CIS administration. (A,B) IC50 of A2780 and A2780/DDP cells detected using the MTS assay before and after co-culture with CD163+ TAMs (M2). (C) Statistical analysis graph showing that the IC50 of cisplatin in A2780 and A2780/DDP cells increased by 3.1 and 1.4 times, respectively, after co-culture, and the difference was statistically significant (n=6). *, P<0.05; **, P<0.01; ***, P<0.001. CIS, cisplatin; DDP, cis-diamminedichloroplatinum; IC50, half maximal inhibitory concentration; OD, optical density; TAMs, tumor-associated macrophages.

IC50 of A2780 and A2780/DDP cells after co-culture with CD163+ TAMs

CD163+ TAMs in ascites of patients with epithelial serous ovarian cancer were isolated and cultured in primary culture and then co-cultured with ovarian cancer cell lines A2780 and A2780/DDP. The changes in cisplatin's ability to kill these cells were detected, and the IC50 of cisplatin was increased. The IC50s of the parental strain A2780 and platinum-resistant strain A2780/DDP were 7.16±3.57 and 73.18±3.01 μg/dL, respectively, and the difference was significant, with a resistance factor (RF) value of 10.71 in CD163+ TAMs. After incubation with A2780 and A2780/DDP cells, the IC50s of cisplatin were, respectively, 22.19±5.47 and 102.45±8.34 μg/dL, which increased by 3.1 and 1.4 times, and the difference was significant (*Figure 2A-2C*).

CD163+ TAM-derived exosomes promote the adhesion and migration

The results showed that addition of CD163+ TAM-derived exosomes increased the adhesion ability of EOC cells, while DDP treatment decreased the migration and adhesion of EOC cells. The 2 co-treatments partially offset this effect, and the overall adhesion of the A2780/DDP strain was higher than that of the parental strain. All results were time-dependent (*Figure 3A,3B*). Moreover, addition of CD163+ TAM exosomes increased the invasive ability of cells, which was partially offset by the 2 treatments, and the overall invasive ability of A2780/DDP cells was higher than that of the parental strain (*Figure 3C*).

CD163+ TAM-derived exosomes can promote EMT, CSC phenotype, and MDR

EMT is associated with CSC transformation and cancer progression, and disruption of epithelial cell homeostasis leading to aggressive cancer progression is associated with the loss of epithelial features and the acquisition of a migratory phenotype and is considered to be a key event in malignancy. Similar loss of differentiation by EMT is typically detectable at the tumor-host interface and is thought to enable cells to detach, spread, and ultimately metastasize (30,31). A2780 and A2780/DDP cells were treated with CD163+ TAM-derived exosomes and DDP for 72 h, respectively. The expression of *SNAIL1*, *ZEB1*, and *TWIST1* was significantly increased after treatment with CD163+ TAM-derived exosomes alone. In contrast, *SNAIL1*, *ZEB1*, and *TWIST1* were downregulated after DDP treatment alone, while they were upregulated to varying degrees under the combined action of CD163+ TAM-derived exosomes and DPP. In A2780 cells, treatment with CD163+ TAM-derived exosomes alone reduced the expression of the mesothelial marker *CHD1* (encoding E-cadherin) and increased the expression of *VIM*, while treatment with DDP alone had the opposite effect. The combined action of CD163+ TAM-derived exosomes and DPP generates a counteracting effect, and changes at the genetic level are not obvious. In A2780/DDP cells, the expression of *CHD1* (E-cadherin) did not change

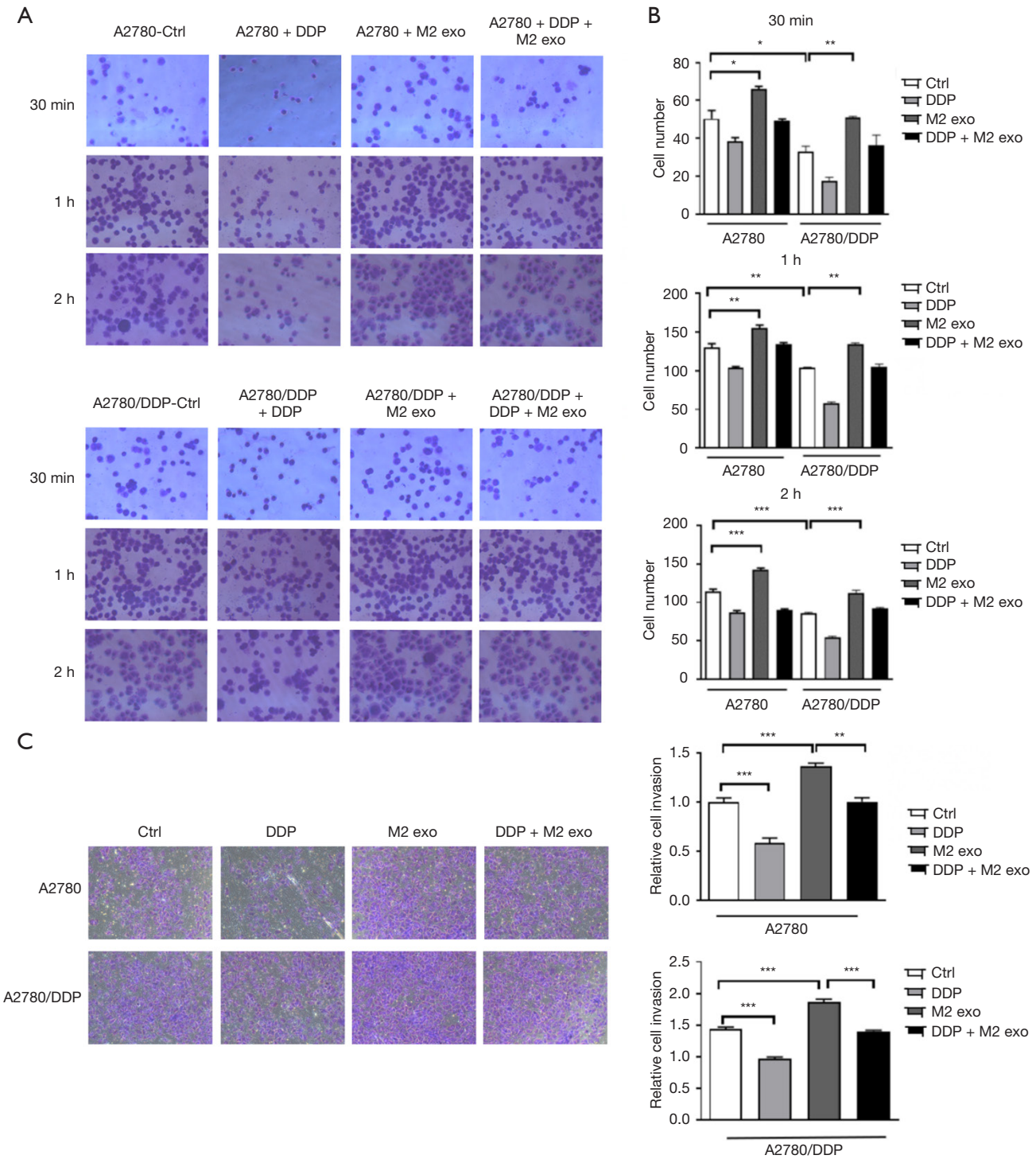

Figure 3 CD163$^+$ TAMs exosomes can promote the adhesion and migration of EOC cells. (A,B) After the addition of CD163$^+$ TAMs (M2 exo), the adhesion ability increased, and DDP administration decreased the cell adhesion. The two kinds of joint treatments had an offset effect, and the overall adhesion of A2780/DDP cells was higher than that of the parental strain. All the results were time dependent. Crystal violet staining, 200×. (C) The two kinds of joint treatments had an offset effect, and the overall adhesion of A2780/DDP cells was higher than that of the parental strain. Crystal violet staining, 400×. All the results were time dependent, and the difference was statistically significant (M2 exo 100 μg, n=3). *, P<0.05; **, P<0.01; ***, P<0.001. DDP, cis-diamminedichloroplatinum; exo, exosomes; EOC, epithelial ovarian cancer; TAMs, tumor-associated macrophages.

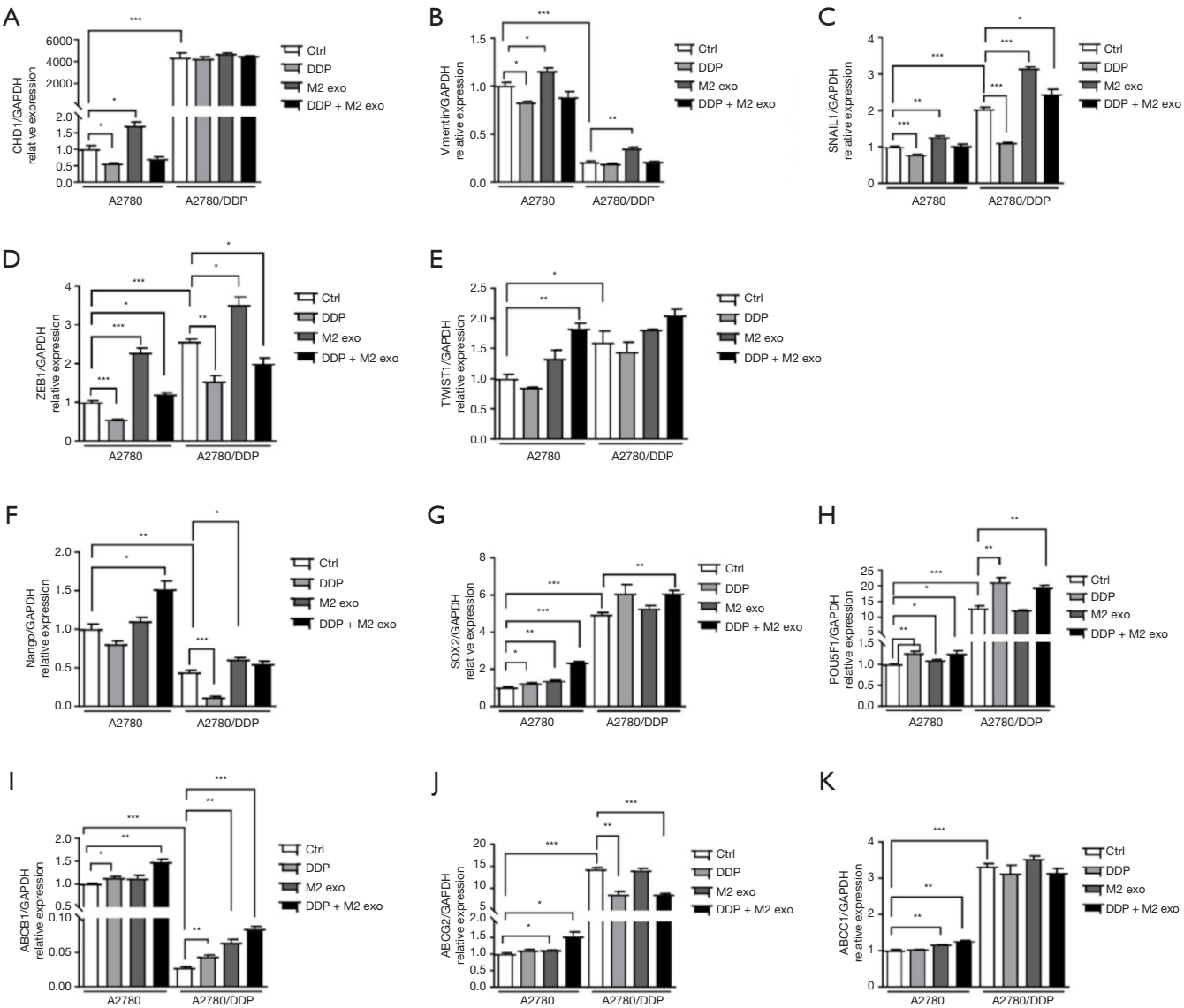

Figure 4 CD163+ TAMs exosomes can promote EMT, CSC characteristics, and MDR expression in EOC cells. (A-E) Expression of EMT transcription factors *SNAIL1*, *ZEB1*, and *TWIST1* and the epithelial signature marker *CHD1* (the gene encoding E-cadherin protein) after 72 h of treatment with CD163+ TAM exosomes also changes the expression of the mesothelial marker Vimentin. (F-H) Changes in the expression of CSC markers *Nango*, *SOX2*, and *POU5F1*. (I-K) Changes in the expression of MDR markers *ABCB1*, *ABCG2* and *ABCC1* (exo 100 μg, n=6). *, P<0.05; **, P<0.01; ***, P<0.001. CSC, cancer stem cell; DDP, cis-diamminedichloroplatinum; EMT, epithelial-mesenchymal transition; EOC, epithelial ovarian cancer; exo, exosomes; MDR, multidrug resistance; TAMs, tumor-associated macrophages.

significantly, while the expression of *VIM* increased, which had little relationship with DDP (*Figure 4A-4E*).

Cells with different molecular signatures within the same tumor also respond differently to anticancer therapy, which leads to drug resistance (32). The expression of *Nango*, *SOX2*, and *POU5F1* slightly increased in A2780 cells after DDP treatment alone. Similar to A2780 cells, the expression of these 3 CSC markers in A2780/DDP cells increased under both conditions, indicating that the 2 had synergistic effects, and the difference was statistically significant (*Figure 4F-4H*).

CSCs express high levels of the ATP-binding cassette (ABC) transporter, which acts as a unidirectional cellular pump and induces cell resistance to chemotherapeutic drugs

by increasing drug efflux and reducing the amount of drug accumulated in cells (33-35). The expression of MDR genes *ABCB1*, *ABCG2*, and *ABCC1* increased slightly in both A2780 and A2780/DDP cells after treatment with $CD163^+$ TAM exosomes for 72 h. The expression of *ABCB1*, *ABCG2*, and *ABCC1* in A2780 cells increased slightly after DDP treatment, and the change was significant. TAM exosomes and DDP in combination had synergistic effects (*Figure 4I-4K*).

Differential expression of ADAMTS6 between $CD163^+$ TAMs and M0

$CD163^+$ TAMs were used as the experimental group and peripheral blood M0 mononuclear cells were used as the control group. The miRNA transcriptome differences between the 2 groups were compared and analyzed using gene chip technology. There was significantly high expression of miR-221-3p (105 times), miR-132-3P (71 times), and miR-708-5P (76 times) in TAMs. Additionally, target gene prediction and GO analysis were performed, and the corresponding target genes of miR-221-3p, miR-132-3P, and miR-708-5P were found to be *ADAMTS6*, *SMAD4*, and *ATXNTL1*, respectively (*Figure 5A*). The results of the luciferase assay conducted by Xie *et al.* confirmed that miR-221-3p directly inhibited c by binding to its 3'-untranslated region (36). The results of the TCGA database analysis showed that the expression of *ADAMTS6* was downregulated 0.6- and 0.8-fold in ovarian cancer peritoneal metastases compared with ovarian cancer low-potential malignant tissues (GSE 9891, 2 probes). Compared with normal ovarian tissue, ovarian cancer tissue showed a 0.5-fold decrease in *ADAMTS6* expression (GTEx), suggesting that this gene may function as a tumor suppressor in ovarian tissue (*Figure 5B*).

Studies have shown that miR-221-3p is associated with proliferation, altered heparin, telomerase activity, evasion of cell death, promotion of angiogenesis, and induction of migration and invasion (37-42). Our results showed that *ADAMTS6* expression in A2780/DDP cells was lower than that in A2780 cells, and $CD163^+$ TAM exosomes could downregulate *ADAMTS6* expression in A2780/DDP cells ($P<0.01$) (*Figure 5C*). Furthermore, compared with M0 exosomes, the mRNA level of miR-221-3p in $CD163^+$ TAM exosomes was increased, and the difference was statistically significant ($P<0.01$) (*Figure 5D*). Transfection of miR-221-3p mimic or control mimic into A2780 and A2780/DDP cells and *ADAMTS6* protein levels in these 2 cell lines were determined by Western blotting, which indicated that miR-221-3p can negatively regulate the expression of *ADAMTS6* protein, and the effect was more apparent in A2780/DDP cells (*Figure 5E*).

Effect of miR-221-3p mimics/inhibitor on cisplatin resistance

To verify whether miR-221-3p is related to cisplatin resistance, we used miR-221-3p mimics/inhibitor to transiently transfect ovarian cancer cell lines to detect the changes in the IC50 of cisplatin. The experimental results showed that miR-221-3p mimics increased the IC50 of cisplatin in A2780 and A2780/DDP cells (1.53- and 1.38-fold, respectively), while miR-221-3p inhibitor decreased the IC50 of cisplatin in A2780 and A2780/DDP cells (0.51- and 0.47-fold, respectively), and these differences were statistically significant (*Figure 6*).

Overexpression of ADAMTS6 reverses cisplatin resistance in EOC cells

To further observe whether the promoting effect of $CD163^+$ TAMs on the drug resistance of A2780 and A2780/DDP cells was reversed after blocking the *AKT* signaling pathway, *ADAMTS6* plasmid was transfected into A2780 and A2780/DDP cells, and the IC50 of cisplatin-treated cells decreased by 0.73- and 0.49-fold in the 2 cell lines, respectively (*Figure 7*).

ADAMTS6 and clinicopathological factors in EOC patients

To verify the expression of *ADAMTS6* in ovarian cancer and to study the relationship between *ADAMTS6* and the occurrence and progression of ovarian cancer, we used Western blotting to detect the expression of *ADAMTS6* in benign tumor tissue and peritoneal metastatic malignant tumor tissue. We found that *ADAMTS6* expression decreased significantly (*Figure 8A,8B*). To explore the correlation between *ADAMTS6* expression level and the clinicopathological factors of patients, we used IHC to detect *ADAMTS6* protein expression in ovarian cancer tissues. Moreover, we analyzed the relationship between *ADAMTS6* expression level and patient age in EOC tissues of 160 patients with complete clinical data, including tumor size, pathological grade, pathological stage, lymph node, and distant metastasis correlation. Immunohistochemical was used to detect *ADAMTS6* protein expression in ovarian cancer cases (*Figure 8C*). The results showed that *ADAMTS6* expression level was significantly correlated with ovarian cancer stage and age (*Tables 2,3*). Patients with relatively low expression of *ADAMTS6* had a shorter overall

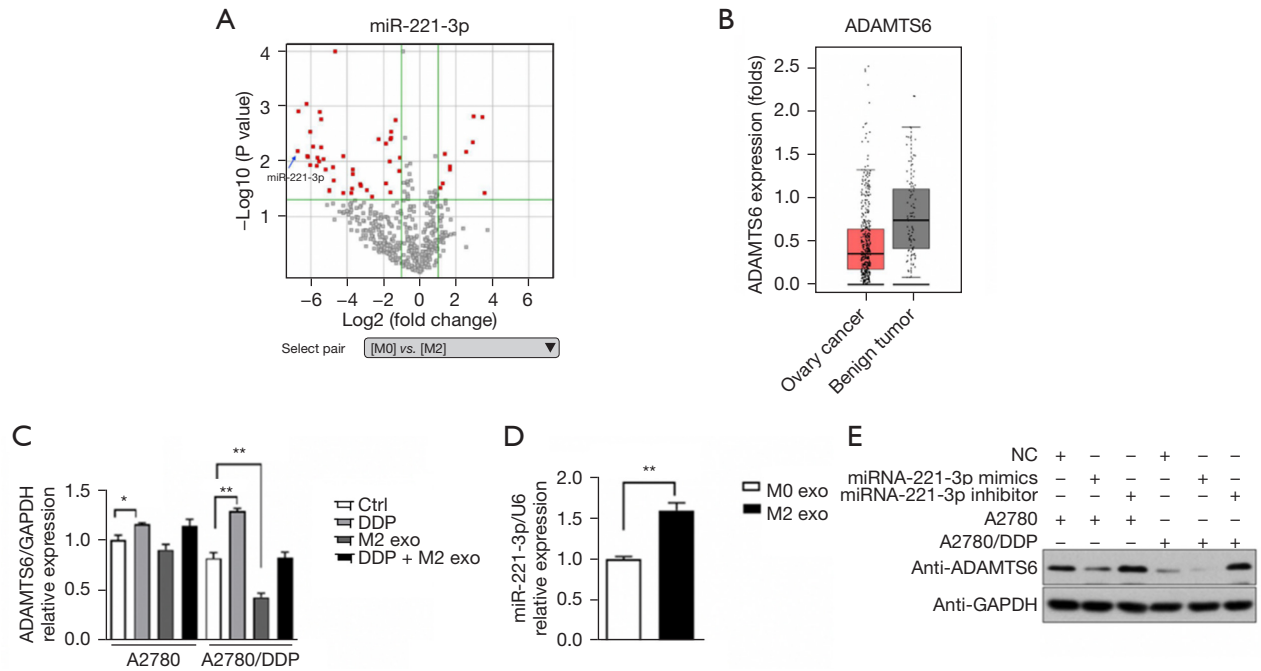

Figure 5 Expression of miR-221-3p and *ADAMTS6*. (A) Differences in the results of microarray analysis of M0 and M2 (CD163+ TAMs) cells. Volcano plot of gene analysis: miR-221-3p was highly expressed in M0 and M2 (CD163+ TAMs) cells (FC =105.22828, P=0.064). (B) *ADAMTS6* expression in ovarian cancer cells and benign lesions derived from TCGA database (ovarian cancer =426, benign tumor =85). (C) CD163+ TAM exosomes (M2 exo) decreased *ADAMTS6* expression after co-culture with A2780/DDP cells. (D) The mRNA level of miR-221-3p was increased in CD163+ TAM exosomes (M2 exo) compared to M0 exo. (E) A2780 and A2780/DDP cells were transfected with miR-221-3p mimics or inhibitors and their respective negative controls. After 72 h of incubation, *ADAMTS6* protein levels were determined by Western blotting. MiR-221-3p negatively regulated *ADAMTS6* protein expression (exo 100 μg, n=6). *, P<0.05; **, P<0.01. Ctrl, control; DDP, cis-diamminedichloroplatinum; exo, exosomes; FC, fold change; NC, negative control.

survival. The median survival rate was 73.95 months, while the median survival rate in the *ADAMTS6* high expression group was 91.13 months, and the difference was statistically significant (*Figure 8D,8E*).

CD163+ TAM exosomes downregulate the expression of ADAMTS6

AKT is a serine/threonine kinase that phosphorylates and regulates downstream effector molecules and plays an important role in regulating cell growth, proliferation, survival, genome stability, glucose metabolism, neovascularization, and activation of EMT transcription factors (43-46). To further verify that CD163+ TAM exosomes promote the proliferation, migration, drug resistance, and EMT progression of A2780 and A2780/DDP cells, the AKT signaling pathway was activated, and the expression of transcription factors was increased depending on the downregulation of *ADAMTS6* protein. The phosphorylation levels of *ADAMTS6* and its downstream *AKT* protein were detected by Western blotting after co-culture of CD163+ TAM exosomes with A2780 and A2780/DDP cells for 72 h. The results showed that CD163+ TAM exosomes could inhibit *ADAMTS6* expression and activate the phosphorylation of its downstream molecule to increase the expression of EMT transcription factors *ZEB1* and *SNAIL1* and the interstitial marker *VIM*. In the presence of DDP, the magnitude of the trend was reduced, while treatment with DDP alone had the opposite effect on cells (*Figure 9*).

TGF-β1/EGFR-AKT is involved in ADAMTS6-mediated EMT

AKT is affected by a variety of extracellular stimuli, such as growth factors, dysregulation of specific proteins, and

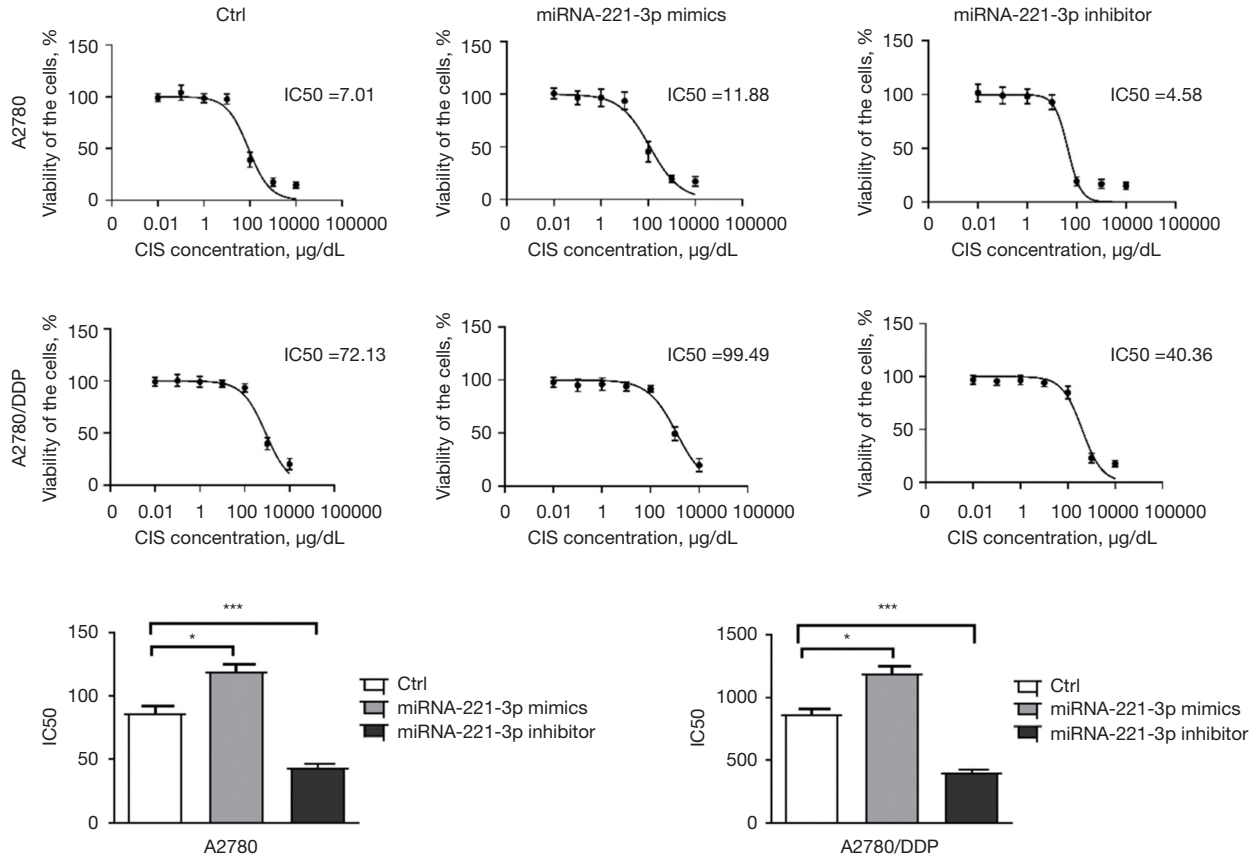

Figure 6 miR-221-3p mimics significantly increased CIS resistance in A2780 and A2780/DDP cells, while miR-221-3p inhibitor decreased CIS resistance in A2780 and A2780/DDP cells (n=3). *, P<0.05; ***, P<0.001. CIS, cisplatin; Ctrl, control; DDP, cis-diamminedichloroplatinum; IC50, half maximal inhibitory concentration.

certain tumor suppressors, which may affect the expression of EMT transcription factors and EMT induction. Epidermal growth factor (EGF) activates the *PI3K/AKT* signaling pathway through the EGF receptor family, and the *TGF-β1/AKT* signaling pathway is also an important regulatory pathway in EMT. The experimental results showed that following the transfection of *ADAMTS6* plasmid into A2780 cells: (I) *ADAMTS6* was overexpressed; (II) *TGF-β1* expression was decreased; (III) *EGFR* expression increased, while phosphorylated *EGFR* (p*EGFR*) expression decreased; (IV) *AKT* expression did not change significantly, but phosphorylated *AKT* (p*AKT*) expression decreased; (V) the expression of *SNAIL1*, *ZEB1*, and *VIM* decreased. Compared with A2780 cells, *ADAMTS6* protein expression was significantly decreased in A2780/DDP cells, which correlated with the RNA level. The protein expression levels of *TGF-β1/EGFR/AKT* pathway proteins were also different between the 2 cell lines. After transfection of the *ADAMTS6* plasmid into A2780/DDP cells, *ADAMTS6* protein and *TGF-β1/EGFR-AKT* signaling pathway expression of *TGF-β1*, p*EGFR/EGFR*, p*AKT/AKT*, *SNAIL1*, *ZEB1*, *VIM*, and other proteins had the same trend as that observed in A2780 cells (*Figure 10A,10B*).

Discussion

Cisplatin is one of the first metal-based chemotherapy drugs. It has been reported that there are approximately $2 billion in platinum-based anticancer drugs worldwide, and almost 50% of all patients are treated with cisplatin (47,48). Cisplatin exerts its anticancer activity through multiple mechanisms, but its most acceptable mechanism involves DNA damage by interacting with purines on DNA, activating multiple signal transduction pathways and ultimately leading to apoptosis (49,50). Resistance

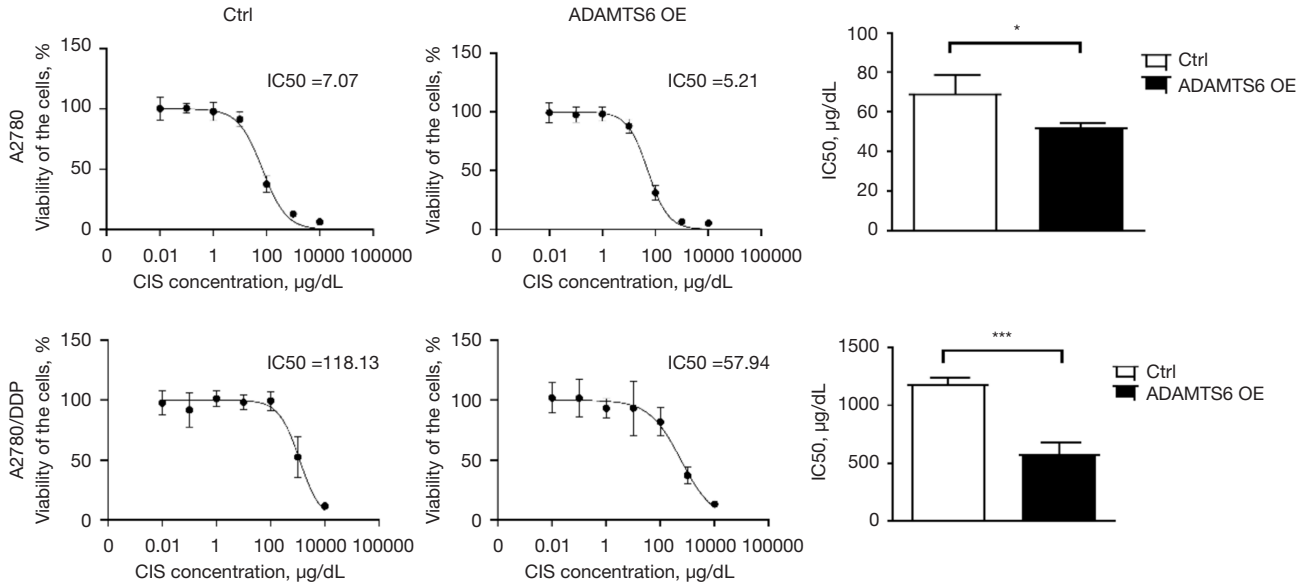

Figure 7 The effect of *ADAMTS6* plasmid transfection into A2780 and A2780/DDP cells on CIS resistance. The IC50 of CIS (μg/dL) decreased significantly compared with the control group (n=3). *, P<0.05; ***, P<0.001. CIS, cisplatin; Ctrl, control; DDP, cis-diamminedichloroplatinum; OE, overexpression.

to cisplatin depends on factors such as reduced drug accumulation, drug inactivation by binding to different proteins, increased DNA repair, altered apoptosis signaling proteins, stemness and EMT Increased capacity, as well as interaction with TME cells (macrophages, T cells, adipocytes, fibroblasts, endothelial cells, migratory hematopoietic cells, stem cells, etc.) (51-55).

As the most abundant inflammatory cell group in the TME, TAMs exist in two subtypes with completely different functions: M1 mainly promotes tumor immunity and inhibits tumorigenesis; M2 mainly promotes tumor growth and metastasis (56-59). Current studies have confirmed that TAMs (M2) can directly inhibit $CD4^+$/$CD8^+$ T cells by promoting tumor angiogenesis, inhibiting apoptosis pathway, mediating immunosuppression. The activity of cells and the secretion of some chemokines to recruit regulatory T cells (Treg cells) cause chemotherapy resistance. Chemotherapy drugs (cisplatin, carboplatin, paclitaxel, doxorubicin, etc.) can also induce M2 polarization in TAMs and increase the tumor-promoting effect, leading to further chemotherapy resistance (60,61).

Lan *et al.* found that high CD163/CD68 ratio in EOC was associated with high tumor grade, and the platinum-resistant recurrence rate was higher in the high CD163/CD68 ratio group, suggesting that macrophage polarization to M2 may be associated with relapse type-related disease in ovarian cancer (platinum-resistant relapse) (24). In the study by Niino *et al.*, cases of angioimmunoblastic T-cell lymphoma (AITL) with a higher infiltration density of CD163-positive macrophages had poorer overall survival and increased CD163/CD68 ratio was associated with poor prognosis (62).

Our experimental results showed that the proportion of $CD163^+$ TAM in total macrophages in ascites of ovarian cancer patients was significantly higher than that in peritoneal lavage fluid of benign ovarian cysts. Secreted exosomes induce ovarian cancer cell lines Resistance of A2780 and A2780/DDP to cisplatin.

A study has found that exosomes secreted by ovarian cancer cells can carry miR-222 to monocytes to induce them to differentiate into M2 macrophages (63). The exosomes of ovarian cancer cells can transmit CD44 to peritoneal mesothelial cells and enhance the invasion and metastasis of ovarian cancer. MiR-21 carried by exosomes of stromal cells can be transmitted to ovarian cancer cells to induce drug resistance; *TGF* carried by exosomes secreted by CAFs-β1 can promote ovarian cancer progression (11,24,64-66). As one of the important stromal cells in the microenvironment of ovarian cancer, a small number of studies have shown that TAMs exosomes have an impact on the malignant biological behavior of ovarian cancer cells (25-28), but the role of exosomes in the signal communication between $CD163^+$

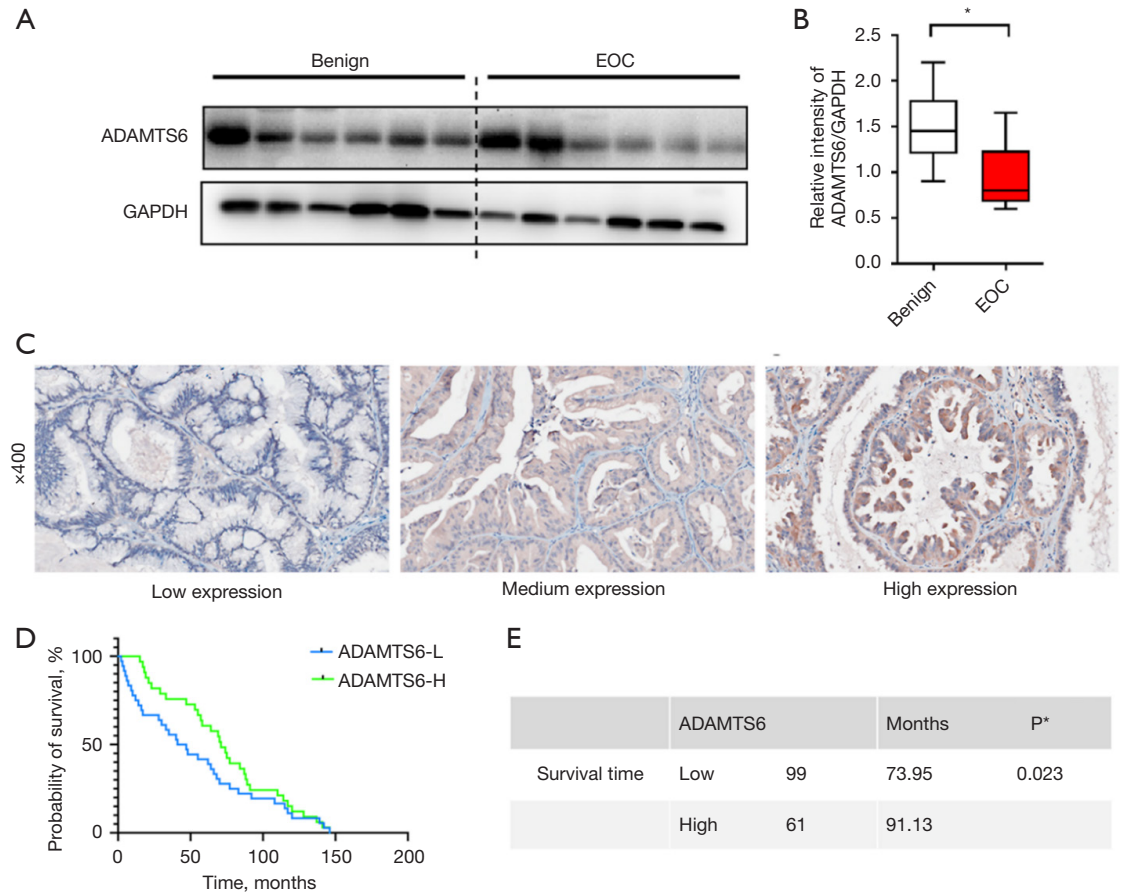

	ADAMTS6		Months	P*
Survival time	Low	99	73.95	0.023
	High	61	91.13	

Figure 8 *ADAMTS6* and clinicopathological factors in EOC patients. (A,B) Western blot detection of *ADAMTS6* protein expression in benign ovarian cysts and EOC (n=6). (C) Immunohistochemical detection of *ADAMTS6* protein expression in ovarian cancer cases. (D,E) Patients with relatively low expression of *ADAMTS6* have a shorter overall survival. *, P<0.05. EOC, epithelial ovarian cancer; L, low; H, high.

TAMs and ovarian cancer cells and their relationship with drug resistance have not been reported yet.

EMT can trigger reversion to a CSC-like phenotype, establishing a link between EMT, CSCs, and drug resistance (67,68). EMT is involved in the *TGF-β*, *Wnt*, Hedgehog (*Hh*), *β-catenin*, *Notch*, *NF-κB*, and *STAT3* signaling pathways (69). Tumor cells in non-CSC subsets can spontaneously undergo EMT-like changes and acquire CSC-like cell surface marker expression, inducing many features of stem cells including self-renewal capacity and antigens associated with CSC phenotypes (70-73). *Oct4*, sex-determining region y-box 2 (*SOX2*), *NANOG*, *CD44* (also known as *Pgp1*), *ALDH1*, *CD133* (also known as *PROM1*), and epithelial cell adhesion molecule (*EpCAM*) (*CD326*) are markers of stem cells (74). Cells with CSC characteristics have stronger resistance to various commonly used chemotherapeutic methods (72-74). CSCs can mediate therapeutic resistance through dormancy, increased DNA repair, drug release, decreased apoptosis, and immunosuppression by interacting with their microenvironmental CSCs (34,75,76). CSCs are often located away from blood vessels and thus are not easily targeted to cells using nanoscale pharmaceutical formulations (77). Stem cells and CSCs express high levels of ATP binding cassette B1 (*ABCB1*) and ATP binding cassette G2 (*ABCG2*). Together with ATP-binding cassette C1 (*ABCC1*), they represent the 3 major MDR genes. CSCs express the ABC transporter, which acts as a unidirectional cellular pump, and high levels may induce cell resistance to chemotherapeutic drugs by increasing drug efflux, thereby attenuating the amount of drug accumulated in cells (34,78,79). EMT that occurs in cancer cells *in vivo* is

Table 2 Association of ADAMTS6 expression with clinicopathological features of ovarian cancer

Parameters	ADAMTS6		
	Low	High	P
Age (years)			0.003*
≤56	46	43	
>56	53	18	
TNM stage			0.000**
I + II	52	50	
III + IV	47	11	
Diameter (cm)			0.108
≤7	40	17	
>7	59	44	
N stage			0.575
Absent	77	45	
Present	22	16	
M stage			0.409
Absent	94	60	
Present	5	1	
Histological grade			0.292
I + II	39	19	
III	60	42	

Differences between groups were assessed by one-way analysis of variance. *, P<0.01; **, P<0.001. TNM, tumor-node-metastasis.

Table 3 Relationship between ADAMTS6 expression and patient characteristics

Characteristics	ADAMTS6 IHC score	
	Mean ± SD	P
Age (years)		0.001*
≤56	38.48±31.903	
>56	23.77±23.941	
TNM stage		0.004*
I + II	39.93±31.408	
III + IV	22.39±19.667	
Diameter (cm)		0.081
≤7	26.48±26.265	
>7	34.98±30.830	
N stage		0.974
Absent	32.51±29.791	
Present	31.72±28.251	
M stage		0.228
Absent	32.51±29.791	
Present	17.69±15.313	
Histological grade		0.670
I + II	30.63±30.460	
III	32.70±29.041	
Histological type		0.636
Serous carcinoma	33.60±27.630	
Mucinous carcinoma	31.21±30.384	

*, P<0.01. IHC, immunohistochemistry; TNM, tumor-node-metastasis; SD, standard deviation.

associated with the activation of a relatively small group of transcription factors (35) termed "EMT-inducing transcription factors" (EMT-TFs), which are divided into 3 distinct protein families: *SNAIL* (including *SNAIL1* and Slug; also known as *SNAIL1* and *SNAIL*), *ZEB* (including *ZEB1* and *ZEB2*), and the basic helix-loop-helix (including *TWIST1*, *TWIST2*, and *TCF3*) family (80). These master regulators of the EMT program regulate the transcription of EMT-related genes through promoter activation or repression, with the end result being the repression of genes associated with epithelial phenotypes to varying degrees. For example, genes encoding E-cadherin and cytokeratin and genes associated with the mesenchymal cell phenotype were upregulated, including those encoding *N-cadherin*, fibronectin, and *VIM* (81). Based on the above research, this experiment selected CSC marker molecules *POU5F1*, *Nango*, and *SOX2*; EMT-TFs *SNAIL1*, *ZEB1*, and *TWIST1*; the epithelial characteristic marker *CHD1*; the mesothelial characteristic marker VIM; and stem cell-expressed MDR genes *ABCB1*, *ABCG2*, and *ABCC1* as research molecules for RT-PCR detection of $CD163^+$ TAM exosomes after co-culture with EOC cell lines A2780 and A2780/DDP. Changes in the expression of the above markers are intended to elucidate the EMT of $CD163^+$ TAMs to ovarian cancer cells and the triggered CSC-phenotypic changes, MDR resistance, and other processes. The experimental results preliminarily showed that after DDP treatment alone, the expression of *POU5F1* and *SOX2* increased slightly, which may be due to the process of cell adaptation to chemotherapy drug treatment. The process of

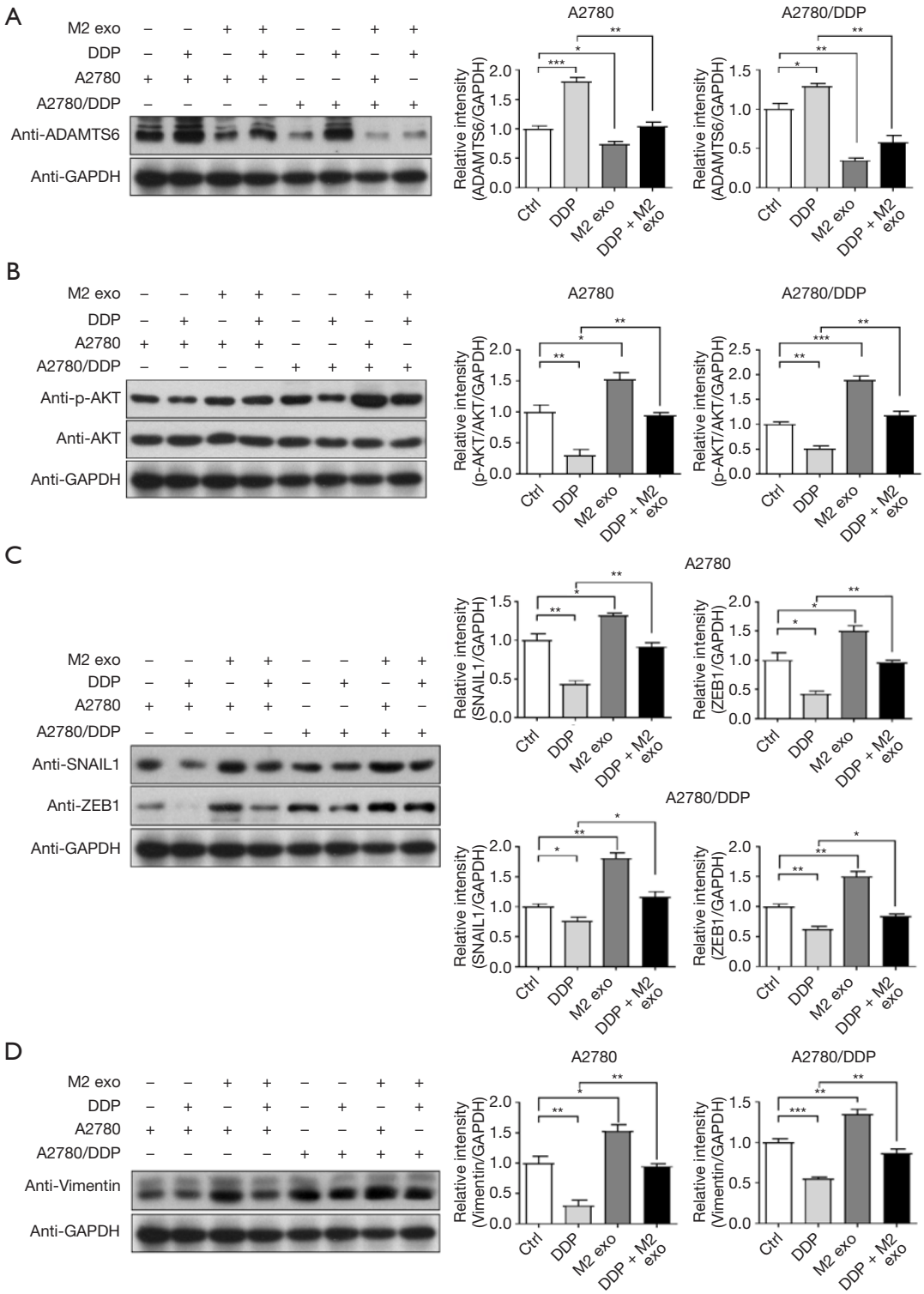

Figure 9 CD163$^+$ TAMs exosomes (M2 exo) inhibited *ADAMTS6* expression, activated the phosphorylation of its downstream molecule *AKT*, and increased the expression of EMT transcription factors *ZEB1*, *SNAIL1*, and *VIM*, and the difference was statistically significant (exo 100 μg, n=6). *, P<0.05; **, P<0.01; ***, P<0.001. DDP, cis-diamminedichloroplatinum; exo, exosomes; EMT, epithelial-mesenchymal transition; TAMs, tumor-associated macrophages; *VIM*, Vimentin.

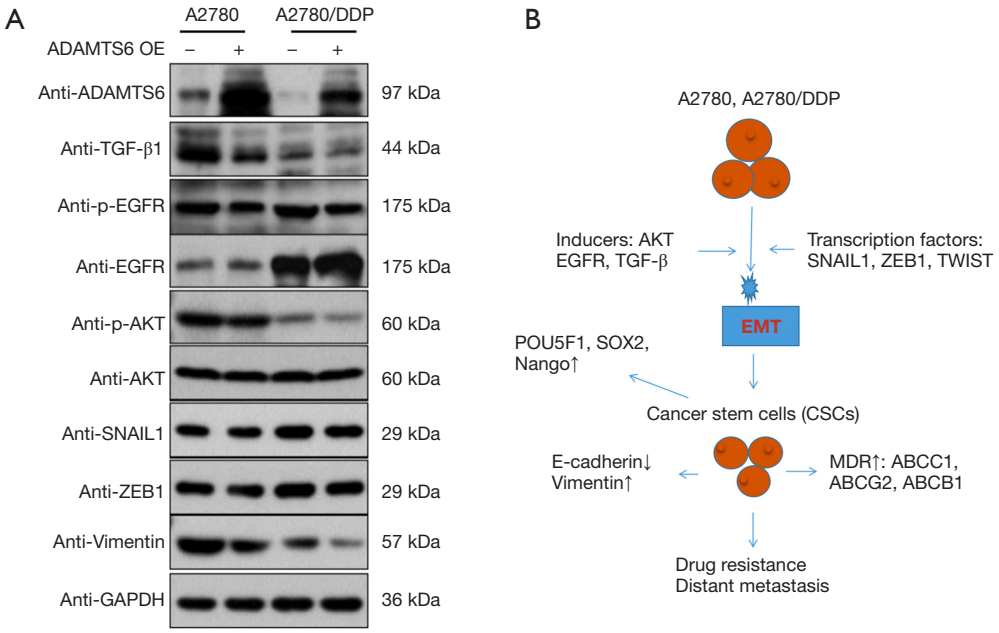

Figure 10 *TGF-β1/EGFR* AKT signaling pathway is involved in *ADAMTS6*-mediated EMT of ovarian cancer cells A2780 and A2780/DDP. (A) Overexpression of *ADAMTS6* affects *TGF-β1* expression in A2780 and A2780/DDP cells and the *EGFR-AKT* signaling pathway. The expression of p*EGFR/EGFR*, p*AKT/AKT* protein, EMT-related molecules *SNAIL1* and *ZEB1*, and mesothelial marker Vimentin. (B) Schematic diagram of the relationship between CSCs, EMT, and tumor biological behavior. CSCs, cancer stem cells; DDP, cis-diamminedichloroplatinum; EMT, epithelial-mesenchymal transition; OE, overexpression; MDR, multidrug resistance; pEGFR, phosphorylated EGFR; pAKT, phosphorylated AKT.

CSC-phenotypic transition, together with CD163$^+$ TAMs, produced additive effects. Cisplatin itself did not trigger EMT induced by the increased expression of EMT-TFs, while CD163$^+$ TAM exosomes could significantly increase the expression of EMT-TFs in A2780 cells. The expression of MDR genes *ABCB1*, *ABCG2*, and *ABCC1* were slightly increased after treatment with CD163$^+$ TAM exosomes and DDP, in A2780 and A2780/DDP respectively. After treatment with CD163$^+$ TAM exosomes alone, the expression of *CHD1* in A2780 cells was decreased, and the expression of *VIM* was increased in both cell lines, indicating that they may have undergone changes during EMT.

Gene-chip analysis results indicated that the expression of miR-221-3p in CD163$^+$ TAMs was increased significantly (105-fold). Target gene prediction and GO analysis showed that the corresponding target gene was *ADAMTS6*. Studies have shown that miR-221-3p is associated with proliferation, altered heparin, telomerase activity, evasion of cell death, and promotion of angiogenesis, and supports EMT in BC by over activating *RAS/ERK* signaling to induce migration and invasion (40-43). The results of a luciferase assay performed by Xie *et al.* confirmed that miR-221-3p directly inhibited *ADAMTS6* by binding to its 3'-untranslated region, whereas high expression of *ADAMTS6* is associated with favorable clinical outcomes in BC (36). In contrast, *ADAMTS6* expression was associated with poor prognosis in PRL tumors, esophageal cancer, myeloma, and pancreatic cancer (82,83). Luu *et al.* showed that *AGR2* downregulated *ADAMTS6* and increased *VEGFA* mRNA expression, which was consistent with *EGFR*-mutant non-small cell lung cancer response to gefitinib or erlotinib, and was highly correlated with resistance to *EGF* receptor tyrosine kinase inhibitors (*EGFR*-TKIs) (84). The results of this experiment showed that CD163$^+$ TAM exosomes highly expressed miR-221-3p, and *ADAMTS6* was negatively regulated by miR-221-3p in A2780 and A2780/DDP cells. *In vitro* results confirmed that miR-221-3p mimics caused an increase in A2780 and A2780/DDP cisplatin resistance, and miR-221-3p inhibitor caused a decrease in A2780 and A2780/DDP cisplatin resistance. The results support that miR-221-3p can mediate cisplatin in ovarian tumors, conferring

platinum resistance. The expression of *ADAMTS6* in ovarian cancer tissues was lower than that in benign ovarian cysts. Additionally, the expression level of *ADAMTS6* was significantly correlated with ovarian cancer stage, age, and overall survival. *ADAMTS6* expression is lower in ovarian cancer patients over 56 years old and TNM stage III–IV. Patients with relatively low *ADAMTS6* expression have shorter overall survival. The median survival rate was 73.95 months, while that of the *ADAMTS6* high expression group was 91.13 months, and the difference was statistically significant. It is suggested that *ADAMTS6* plays the role of a suppressor in ovarian tumors. *AKT* is a serine/threonine kinase that phosphorylates and regulates downstream effector molecules, and is involved in the regulation of cell growth, proliferation, survival, genome stabilization, glucose metabolism, neovascularization, and activation of EMT transduction (43-46). Recent studies have highlighted the role of the *AKT* signaling pathway in inducing EMT in different cancer cells (84-90). In our study, p*AKT/AKT-SNAIL1-ZEB1-VIM* expression was detected after co-culture of $CD163^+$ TAM exosomes with A2780 and A2780/DDP cells. The results showed that $CD163^+$ TAM exosomes downregulated *ADAMTS6* expression, increased *AKT* phosphorylation, upregulated EMT transcription factors *SNAIL1* and *ZEB1*, and increased the expression of *VIM*. To further verify the role of *ADAMTS6* in cisplatin resistance in ovarian cancer, we designed reversal experiments by transfecting *ADAMTS6* plasmid into A2780 and A2780/DDP cells and detected the IC50 after cisplatin treatment, which decreased by 0.73- and 0.49-fold in A2780 and A2780/DDP cells, respectively. It was further demonstrated that miR-221-3p caused ovarian cancer drug resistance by downregulating *ADAMTS6*. *TGF-β* signaling is one of the most typical pathways involved in EMT induction, occurring through the induction of other signals including *ERK* and *PI3K/AKT* by *TGF-β* (91-93). *TGF-β1* is secreted in the form of L-*TGF-β1* (latent *TGF-β1*), which constitutes a link between *TGF-β1* and latency associated peptide (LAP) (94). On the cell surface, L-*TGF-β1* can be processed in various ways to excise LAP and release biologically active *TGF-β1* (94-97). *TSP1* is an important physiological regulator of *TGF-β1*. The LAP in L-*TGF-β1* recognizes and binds the KRFK sequence in *TSP1* to form the *TSP1*/L-*TGF-β1* complex, and then the CSVTCG sequence in *TSP1* binds to CD36 and releases the active *TGF-β1* factor (98). The auxiliary domains of all ADAMTS enzymes are known to contain a 50 amino acid thrombospondin-like repeat (TSR), similar to the type I repeats of thrombospondin 1 and 2 (*TSP1*) (99). *TSP1* is a natural angiogenesis inhibitor, which can bind to glycoprotein CD36 via CSVTCG and GVQXR functional sequences (100,101). Chen *et al.* used *TSR2–3*-glutathione S-transferase fusion protein (*GST*) fusion protein, *TSP1* [447–452] synthetic peptide, and anti-CD36 antibody to test the antagonism of L-*TGF-β1* activation secreted by mouse alveolar macrophages (AMs) (98). The results revealed that *TSP1* functional fragment and anti-CD36 activation of L-*TGF-β1* secreted by AMs was induced by bleomycin-induced lung injury (102). From this we hypothesized that *ADAMTS6* could be inhibited by the CSVTCG sequence in the included TSR. The activation of L-*TGF-β1* and the release of *TGF-β1* in turn inhibit the activity of the downstream molecule *AKT*. The experimental results show that *ADAMTS6* can effectively reduce the expression of *TGF-β1* and the phosphorylation of *AKT*, and thereby inhibit the *AKT* pathway. The expression of EMT transcription factors *SNAIL1* and *ZEB1* in the *AKT* pathway was increased, and the expression of *VIM* was also increased. Thus, it was verified that *ADAMTS6* could inhibit the *AKT* pathway and EMT process by inhibiting the upstream molecule *TGF-β* of the *AKT* pathway. *EGFR* is also an important upstream activator of *AKT* (99,103,104). Activation of downstream signaling from *EGFR* depends on both the increased abundance of *EGFR* and its phosphorylation. Studies have confirmed that both *ADAMTS1* and *ADAMTS8* can affect their phosphorylation levels (105,106). Our experimental results showed that *ADAMTS6* overexpression had no effect on the expression abundance of *EGFR* in EOC cells, but reduced its phosphorylation level and inhibited the *AKT* pathway. In conclusion, *ADAMTS6* can inhibit the expression of p*EGFR* and *TGF-β1* in ovarian cancer cells A2780 and A2780/DDP, then, inhibit the *AKT* pathway. The expression of EMT transcription factors *SNAIL1* and *ZEB1*, the downstream molecules of *AKT* pathway, increased, and the expression of mesothelial marker *VIM*. Subsequently, the phenomenon of EMT in A2780 and A2780/DDP cells was reversed. Thus, the transformation to CSC like phenotype and the subsequent expression of MDR genes were reduced, and finally the cisplatin resistance of ovarian cancer cells was reversed.

In summary, the experimental results showed that in the ascites of patients with ovarian cancer, the proportion of $CD163^+$ TAMs of the total macrophages was significantly higher than that of the peritoneal lavage fluid of benign ovarian cysts. The secreted exosomes can induce

cisplatin resistance in ovarian cancer cell lines A2780 and A2780/DDP. CD163+ TAM exosomes can increase the proliferation, adhesion, and invasion of ovarian cancer cells, and downregulate the expression of *ADAMTS6* in ovarian cancer cells by targeting miR-221-3p, which activates the *AKT* signaling pathway and promotes EMT and CSCs, MDR processes are involved in the occurrence of cisplatin resistance in ovarian cancer. Overexpression of ADAMTS can inhibit its upstream activators *EGFR* and *TGF-β1* to inhibit the *AKT* signaling pathway, thereby inhibiting the EMT process and reversing drug resistance.

Acknowledgments

Funding: This work was supported by the National Science Foundation of China (No. 81602278).

Footnote

Reporting Checklist: The authors have completed the MDAR reporting checklist. Available at https://atm.amegroups.com/article/view/10.21037/atm-22-4267/rc

Data Sharing Statement: Available at https://atm.amegroups.com/article/view/10.21037/atm-22-4267/dss

Conflicts of Interest: All authors have completed the ICMJE uniform disclosure form (available at https://atm.amegroups.com/article/view/10.21037/atm-22-4267/coif). The authors have no conflicts of interest to declare.

Ethical Statement: The authors are accountable for all aspects of the work in ensuring that questions related to the accuracy or integrity of any part of the work are appropriately investigated and resolved. The study was conducted in accordance with the Declaration of Helsinki (as revised in 2013). The study was approved by the Ethics Committee of Shanghai First Maternity and Infant Hospital, Tongji University School of Medicine (approval No. [KS1937]), and informed consent was taken from all the patients.

References

1. Bast RC Jr, Hennessy B, Mills GB. The biology of ovarian cancer: new opportunities for translation. Nat Rev Cancer 2009;9:415-28.
2. Bray F, Ferlay J, Soerjomataram I, et al. Global cancer statistics 2018: GLOBOCAN estimates of incidence and mortality worldwide for 36 cancers in 185 countries. CA Cancer J Clin 2018;68:394-424.
3. Webb PM, Jordan SJ. Epidemiology of epithelial ovarian cancer. Best Pract Res Clin Obstet Gynaecol 2017;41:3-14.
4. Goff BA, Mandel LS, Melancon CH, et al. Frequency of symptoms of ovarian cancer in women presenting to primary care clinics. JAMA 2004;291:2705-12.
5. Thibault B, Castells M, Delord JP, et al. Ovarian cancer microenvironment: implications for cancer dissemination and chemoresistance acquisition. Cancer Metastasis Rev 2014;33:17-39.
6. Kim J, Bae JS. Tumor-Associated Macrophages and Neutrophils in Tumor Microenvironment. Mediators Inflamm 2016;2016:6058147.
7. Menen RS, Hassanein MK, Momiyama M, et al. Tumor-educated macrophages promote tumor growth and peritoneal metastasis in an orthotopic nude mouse model of human pancreatic cancer. In Vivo 2012;26:565-9.
8. Wyckoff J, Wang W, Lin EY, et al. A paracrine loop between tumor cells and macrophages is required for tumor cell migration in mammary tumors. Cancer Res 2004;64:7022-9.
9. Cioroianu AI, Stinga PI, Sticlaru L, et al. Tumor Microenvironment in Diffuse Large B-Cell Lymphoma: Role and Prognosis. Anal Cell Pathol (Amst) 2019;2019:8586354.
10. Reinartz S, Schumann T, Finkernagel F, et al. Mixed-polarization phenotype of ascites-associated macrophages in human ovarian carcinoma: correlation of CD163 expression, cytokine levels and early relapse. Int J Cancer 2014;134:32-42.
11. Au Yeung CL, Co NN, Tsuruga T, et al. Exosomal transfer of stroma-derived miR21 confers paclitaxel resistance in ovarian cancer cells through targeting APAF1. Nat Commun 2016;7:11150.
12. Nieto MA, Huang RY, Jackson RA, et al. EMT: 2016. Cell

2016;166:21-45.
13. Appert-Collin A, Hubert P, Crémel G, et al. Role of ErbB Receptors in Cancer Cell Migration and Invasion. Front Pharmacol 2015;6:283.
14. Roskoski R Jr. The ErbB/HER family of protein-tyrosine kinases and cancer. Pharmacol Res 2014;79:34-74.
15. Kelwick R, Desanlis I, Wheeler GN, et al. The ADAMTS (A Disintegrin and Metalloproteinase with Thrombospondin motifs) family. Genome Biol 2015;16:113.
16. Apte SS. A disintegrin-like and metalloprotease (reprolysin type) with thrombospondin type 1 motifs: the ADAMTS family. Int J Biochem Cell Biol 2004;36:981-5.
17. Apte SS. A disintegrin-like and metalloprotease (reprolysin-type) with thrombospondin type 1 motif (ADAMTS) superfamily: functions and mechanisms. J Biol Chem 2009;284:31493-7.
18. Jones GC, Riley GP. ADAMTS proteinases: a multi-domain, multi-functional family with roles in extracellular matrix turnover and arthritis. Arthritis Res Ther 2005;7:160-9.
19. Cal S, López-Otín C. ADAMTS proteases and cancer. Matrix Biol 2015;44-46:77-85.
20. Hurskainen TL, Hirohata S, Seldin MF, et al. ADAM-TS5, ADAM-TS6, and ADAM-TS7, novel members of a new family of zinc metalloproteases. General features and genomic distribution of the ADAM-TS family. J Biol Chem 1999;274:25555-63.
21. Porter S, Scott SD, Sassoon EM, et al. Dysregulated expression of adamalysin-thrombospondin genes in human breast carcinoma. Clin Cancer Res 2004;10:2429-40.
22. Wierinckx A, Auger C, Devauchelle P, et al. A diagnostic marker set for invasion, proliferation, and aggressiveness of prolactin pituitary tumors. Endocr Relat Cancer 2007;14:887-900.
23. Xiao WH, Qu XL, Li XM, et al. Identification of commonly dysregulated genes in colorectal cancer by integrating analysis of RNA-Seq data and qRT-PCR validation. Cancer Gene Ther 2015;22:278-84.
24. Lan C, Huang X, Lin S, et al. Expression of M2-polarized macrophages is associated with poor prognosis for advanced epithelial ovarian cancer. Technol Cancer Res Treat 2013;12:259-67.
25. Takaishi K, Komohara Y, Tashiro H, et al. Involvement of M2-polarized macrophages in the ascites from advanced epithelial ovarian carcinoma in tumor progression via Stat3 activation. Cancer Sci 2010;101:2128-36.
26. Carroll MJ, Kapur A, Felder M, et al. M2 macrophages induce ovarian cancer cell proliferation via a heparin binding epidermal growth factor/matrix metalloproteinase 9 intercellular feedback loop. Oncotarget 2016;7:86608-20.
27. Coward J, Kulbe H, Chakravarty P, et al. Interleukin-6 as a therapeutic target in human ovarian cancer. Clin Cancer Res 2011;17:6083-96.
28. Koblish HK, Hansbury MJ, Bowman KJ, et al. Hydroxyamidine inhibitors of indoleamine-2,3-dioxygenase potently suppress systemic tryptophan catabolism and the growth of IDO-expressing tumors. Mol Cancer Ther 2010;9:489-98.
29. Clear AJ, Lee AM, Calaminici M, et al. Increased angiogenic sprouting in poor prognosis FL is associated with elevated numbers of CD163+ macrophages within the immediate sprouting microenvironment. Blood 2010;115:5053-6.
30. Kalluri R, Weinberg RA. The basics of epithelial-mesenchymal transition. J Clin Invest 2009;119:1420-8.
31. Thiery JP. Epithelial-mesenchymal transitions in development and pathologies. Curr Opin Cell Biol 2003;15:740-6.
32. Chou MY, Hu FW, Yu CH, et al. Sox2 expression involvement in the oncogenicity and radiochemoresistance of oral cancer stem cells. Oral Oncol 2015;51:31-9.
33. Zhou BB, Zhang H, Damelin M, et al. Tumour-initiating cells: challenges and opportunities for anticancer drug discovery. Nat Rev Drug Discov 2009;8:806-23.
34. Dean M, Fojo T, Bates S. Tumour stem cells and drug resistance. Nat Rev Cancer 2005;5:275-84.
35. Dianat-Moghadam H, Heidarifard M, Jahanban-Esfahlan R, et al. Cancer stem cells-emanated therapy resistance: Implications for liposomal drug delivery systems. J Control Release 2018;288:62-83.
36. Xie Y, Gou Q, Xie K, et al. ADAMTS6 suppresses tumor progression via the ERK signaling pathway and serves as a prognostic marker in human breast cancer. Oncotarget 2016;7:61273-83.
37. Garofalo M, Quintavalle C, Romano G, et al. miR221/222 in cancer: their role in tumor progression and response to therapy. Curr Mol Med 2012;12:27-33.
38. Kaboli PJ, Rahmat A, Ismail P, et al. MicroRNA-based therapy and breast cancer: A comprehensive review of novel therapeutic strategies from diagnosis to treatment. Pharmacol Res 2015;97:104-21.
39. Chen WX, Hu Q, Qiu MT, et al. miR-221/222: promising biomarkers for breast cancer. Tumour Biol 2013;34:1361-70.

40. Stinson S, Lackner MR, Adai AT, et al. miR-221/222 targeting of trichorhinophalangeal 1 (TRPS1) promotes epithelial-to-mesenchymal transition in breast cancer. Sci Signal 2011;4:pt5.
41. Gao J, Wei J, Wang Y, et al. A versatile magnetic bead-based flow cytometric assay for the detection of thyroid cancer related hsa-miR-221-3p in blood and tissues. Analyst 2021;146:842-7.
42. Massillo C, Duca RB, Lacunza E, et al. Adipose tissue from metabolic syndrome mice induces an aberrant miRNA signature highly relevant in prostate cancer development. Mol Oncol 2020;14:2868-83.
43. Xie L, Liao Y, Shen L, et al. Identification of the miRNA-mRNA regulatory network of small cell osteosarcoma based on RNA-seq. Oncotarget 2017;8:42525-36.
44. Altomare DA, Testa JR. Perturbations of the AKT signaling pathway in human cancer. Oncogene 2005;24:7455-64.
45. Manning BD, Cantley LC. AKT/PKB signaling: navigating downstream. Cell 2007;129:1261-74.
46. Soltani A, Bahreyni A, Boroumand N, et al. Therapeutic potency of mTOR signaling pharmacological inhibitors in the treatment of proinflammatory diseases, current status, and perspectives. J Cell Physiol 2018;233:4783-90.
47. Hambley TW. Platinum binding to DNA: structural controls and consequences. J Chem Soc Dalton Trans 2001;19: 2711-8.
48. Galanski M, Jakupec MA, Keppler BK. Update of the preclinical situation of anticancer platinum complexes: novel design strategies and innovative analytical approaches. Curr Med Chem 2005;12:2075-94.
49. Ciccarelli RB, Solomon MJ, Varshavsky A, et al. In vivo effects of cis- and trans-diamminedichloroplatinum(II) on SV40 chromosomes: differential repair, DNA-protein cross-linking, and inhibition of replication. Biochemistry 1985;24:7533-40.
50. Jordan P, Carmo-Fonseca M. Molecular mechanisms involved in cisplatin cytotoxicity. Cell Mol Life Sci 2000;57:1229-35.
51. Kelland LR. Preclinical perspectives on platinum resistance. Drugs 2000;59 Suppl 4:1-8; discussion 37-8.
52. Siddik ZH. Cisplatin: mode of cytotoxic action and molecular basis of resistance. Oncogene 2003;22:7265-79.
53. Rocha CRR, Silva MM, Quinet A, et al. DNA repair pathways and cisplatin resistance: an intimate relationship. Clinics (Sao Paulo) 2018;73:e478s.
54. Skowron MA, Melnikova M, van Roermund JGH, et al. Multifaceted Mechanisms of Cisplatin Resistance in Long-Term Treated Urothelial Carcinoma Cell Lines. Int J Mol Sci 2018;19:590.
55. Noy R, Pollard JW. Tumor-associated macrophages: from mechanisms to therapy. Immunity 2014;41:49-61. Erratum in: Immunity. 2014 Nov 20;41(5):866.
56. Caux C, Ramos RN, Prendergast GC, et al. A Milestone Review on How Macrophages Affect Tumor Growth. Cancer Res 2016;76:6439-42.
57. Colegio OR, Chu NQ, Szabo AL, et al. Functional polarization of tumour-associated macrophages by tumour-derived lactic acid. Nature 2014;513:559-63.
58. Biswas SK, Sica A, Lewis CE. Plasticity of macrophage function during tumor progression: regulation by distinct molecular mechanisms. J Immunol 2008;180:2011-7.
59. Curiel TJ, Coukos G, Zou L, et al. Specific recruitment of regulatory T cells in ovarian carcinoma fosters immune privilege and predicts reduced survival. Nat Med 2004;10:942-9.
60. Kryczek I, Zou L, Rodriguez P, et al. B7-H4 expression identifies a novel suppressive macrophage population in human ovarian carcinoma. J Exp Med 2006;203:871-81.
61. Dijkgraaf EM, Heusinkveld M, Tummers B, et al. Chemotherapy alters monocyte differentiation to favor generation of cancer-supporting M2 macrophages in the tumor microenvironment. Cancer Res 2013;73:2480-92.
62. Niino D, Komohara Y, Murayama T, et al. Ratio of M2 macrophage expression is closely associated with poor prognosis for Angioimmunoblastic T-cell lymphoma (AITL). Pathol Int 2010;60:278-83.
63. Ying X, Wu Q, Wu X, et al. Epithelial ovarian cancer-secreted exosomal miR-222-3p induces polarization of tumor-associated macrophages. Oncotarget 2016;7:43076-87.
64. Bhome R, Goh RW, Bullock MD, et al. Exosomal microRNAs derived from colorectal cancer-associated fibroblasts: role in driving cancer progression. Aging (Albany NY) 2017;9:2666-94.
65. Li X, Wang X. The emerging roles and therapeutic potential of exosomes in epithelial ovarian cancer. Mol Cancer 2017;16:92.
66. Nakamura K, Sawada K, Kinose Y, et al. Exosomes Promote Ovarian Cancer Cell Invasion through Transfer of CD44 to Peritoneal Mesothelial Cells. Mol Cancer Res 2017;15:78-92.
67. Komohara Y, Hasita H, Ohnishi K, et al. Macrophage infiltration and its prognostic relevance in clear cell renal cell carcinoma. Cancer Sci 2011;102:1424-31.
68. Thiery JP, Acloque H, Huang RY, et al. Epithelial-

mesenchymal transitions in development and disease. Cell 2009;139:871-90.
69. Roy S, Sunkara RR, Parmar MY, et al. EMT imparts cancer stemness and plasticity: new perspectives and therapeutic potential. Front Biosci (Landmark Ed) 2021;26:238-65.
70. Polyak K, Weinberg RA. Transitions between epithelial and mesenchymal states: acquisition of malignant and stem cell traits. Nat Rev Cancer 2009;9:265-73.
71. Cai Z, Cao Y, Luo Y, et al. Signalling mechanism(s) of epithelial-mesenchymal transition and cancer stem cells in tumour therapeutic resistance. Clin Chim Acta 2018;483:156-63.
72. Brabletz T, Jung A, Spaderna S, et al. Opinion: migrating cancer stem cells - an integrated concept of malignant tumour progression. Nat Rev Cancer 2005;5:744-9.
73. Singh SS, Vats S, Chia AY, et al. Dual role of autophagy in hallmarks of cancer. Oncogene 2018;37:1142-58.
74. Singh A, Settleman J. EMT, cancer stem cells and drug resistance: an emerging axis of evil in the war on cancer. Oncogene 2010;29:4741-51.
75. Zuo ZQ, Chen KG, Yu XY, et al. Promoting tumor penetration of nanoparticles for cancer stem cell therapy by TGF-β signaling pathway inhibition. Biomaterials 2016;82:48-59.
76. Zhao J. Cancer stem cells and chemoresistance: The smartest survives the raid. Pharmacol Ther 2016;160:145-58.
77. Aderetti DA, Hira VVV, Molenaar RJ, et al. The hypoxic peri-arteriolar glioma stem cell niche, an integrated concept of five types of niches in human glioblastoma. Biochim Biophys Acta Rev Cancer 2018;1869:346-54.
78. Visvader JE, Lindeman GJ. Cancer stem cells in solid tumours: accumulating evidence and unresolved questions. Nat Rev Cancer 2008;8:755-68.
79. Cao S, Wang Z, Gao X, et al. FOXC1 induces cancer stem cell-like properties through upregulation of beta-catenin in NSCLC. J Exp Clin Cancer Res 2018;37:220.
80. Xu J, Lamouille S, Derynck R. TGF-beta-induced epithelial to mesenchymal transition. Cell Res 2009;19:156-72.
81. De Craene B, Berx G. Regulatory networks defining EMT during cancer initiation and progression. Nat Rev Cancer 2013;13:97-110.
82. Lamouille S, Xu J, Derynck R. Molecular mechanisms of epithelial-mesenchymal transition. Nat Rev Mol Cell Biol 2014;15:178-96.
83. Lee M, Rodansky ES, Smith JK, et al. ADAMTS13 promotes angiogenesis and modulates VEGF-induced angiogenesis. Microvasc Res 2012;84:109-15.
84. Luu TT, Bach DH, Kim D, et al. Overexpression of AGR2 Is Associated With Drug Resistance in Mutant Non-small Cell Lung Cancers. Anticancer Res 2020;40:1855-66.
85. Huang HN, Huang WC, Lin CH, et al. Chromosome 20q13.2 ZNF217 locus amplification correlates with decreased E-cadherin expression in ovarian clear cell carcinoma with PI3K-Akt pathway alterations. Hum Pathol 2014;45:2318-25.
86. Tang H, Massi D, Hemmings BA, et al. AKT-ions with a TWIST between EMT and MET. Oncotarget 2016;7:62767-77.
87. Visciano C, Liotti F, Prevete N, et al. Mast cells induce epithelial-to-mesenchymal transition and stem cell features in human thyroid cancer cells through an IL-8-Akt-Slug pathway. Oncogene 2015;34:5175-86.
88. Hong KO, Kim JH, Hong JS, et al. Inhibition of Akt activity induces the mesenchymal-to-epithelial reverting transition with restoring E-cadherin expression in KB and KOSCC-25B oral squamous cell carcinoma cells. J Exp Clin Cancer Res 2009;28:28.
89. Hao L, Ha JR, Kuzel P, et al. Cadherin switch from E- to N-cadherin in melanoma progression is regulated by the PI3K/PTEN pathway through Twist and Snail. Br J Dermatol 2012;166:1184-97.
90. Chua HL, Bhat-Nakshatri P, Clare SE, et al. NF-kappaB represses E-cadherin expression and enhances epithelial to mesenchymal transition of mammary epithelial cells: potential involvement of ZEB-1 and ZEB-2. Oncogene 2007;26:711-24.
91. Julien S, Puig I, Caretti E, et al. Activation of NF-kappaB by Akt upregulates Snail expression and induces epithelium mesenchyme transition. Oncogene 2007;26:7445-56.
92. Mortezaee K. Human hepatocellular carcinoma: Protection by melatonin. J Cell Physiol 2018;233:6486-508.
93. Najafi M, Salehi E, Farhood B, et al. Adjuvant chemotherapy with melatonin for targeting human cancers: A review. J Cell Physiol 2019;234:2356-72.
94. Abe M, Oda N, Sato Y, et al. Augmented binding and activation of latent transforming growth factor-beta by a tryptic fragment of latency associated peptide. Endothelium 2002;9:25-36.
95. Annes JP, Chen Y, Munger JS, et al. Integrin alphaVbeta6-mediated activation of latent TGF-beta requires the latent TGF-beta binding protein-1. J Cell Biol 2004;165:723-34.
96. Khalil N, Corne S, Whitman C, et al. Plasmin regulates the activation of cell-associated latent TGF-beta 1 secreted

by rat alveolar macrophages after in vivo bleomycin injury. Am J Respir Cell Mol Biol 1996;15:252-9.
97. Khalil N. TGF-beta: from latent to active. Microbes Infect 1999;1:1255-63.
98. Chen Y, Wang X, Weng D, et al. A TSP-1 functional fragment inhibits activation of latent transforming growth factor-beta1 derived from rat alveolar macrophage after bleomycin treatment. Exp Toxicol Pathol 2009;61:67-73.
99. Wagstaff L, Kelwick R, Decock J, et al. The roles of ADAMTS metalloproteinases in tumorigenesis and metastasis. Front Biosci (Landmark Ed) 2011;16:1861-72.
100. Dawson DW, Pearce SF, Zhong R, et al. CD36 mediates the In vitro inhibitory effects of thrombospondin-1 on endothelial cells. J Cell Biol 1997;138:707-17.
101. Asch AS, Silbiger S, Heimer E, et al. Thrombospondin sequence motif (CSVTCG) is responsible for CD36 binding. Biochem Biophys Res Commun 1992;182:1208-17.
102. Yehualaeshet T, O'Connor R, Begleiter A, et al. A CD36 synthetic peptide inhibits bleomycin-induced pulmonary inflammation and connective tissue synthesis in the rat. Am J Respir Cell Mol Biol 2000;23:204-12.
103. Miquel-Serra L, Serra M, Hernández D, et al. V3 versican isoform expression has a dual role in human melanoma tumor growth and metastasis. Lab Invest 2006;86:889-901.
104. Yonesaka K, Tanizaki J, Maenishi O, et al. HER3 Augmentation via Blockade of EGFR/AKT Signaling Enhances Anticancer Activity of HER3-Targeting Patritumab Deruxtecan in EGFR-Mutated Non-Small Cell Lung Cancer. Clin Cancer Res 2022;28:390-403.
105. Tung SL, Huang WC, Hsu FC, et al. miRNA-34c-5p inhibits amphiregulin-induced ovarian cancer stemness and drug resistance via downregulation of the AREG-EGFR-ERK pathway. Oncogenesis 2017;6:e326.
106. Lu X, Wang Q, Hu G, et al. ADAMTS1 and MMP1 proteolytically engage EGF-like ligands in an osteolytic signaling cascade for bone metastasis. Genes Dev 2009;23:1882-94.

Cite this article as: Zhang X, Wang J, Liu N, Wu W, Li H, Chen J, Guo X. Molecular mechanism of CD163+ tumor-associated macrophage (TAM)-derived exosome-induced cisplatin resistance in ovarian cancer ascites. Ann Transl Med 2022;10(18):1014. doi: 10.21037/atm-22-4267

